Published in final edited form as:
J Comp Neurol. 2014 January 1; 522(1): 36–63. doi:10.1002/cne.23425.

Topographically Organized Projection to Posterior Insular Cortex from the Posterior Portion of the Ventral Medial Nucleus (VMpo) in the Long-tailed Macaque Monkey

A.D. (Bud) Craig
Atkinson Research Laboratory, Barrow Neurological Institute, Phoenix, AZ 85013

Abstract

Prior anterograde tracing work identified somatotopically organized lamina I trigemino- and spino-thalamic terminations in a cytoarchitectonically distinct portion of posterolateral thalamus of the macaque monkey, named the posterior part of the ventral medial nucleus (VMpo; Craig, 2004b). Microelectrode recordings from clusters of selectively thermoreceptive or nociceptive neurons were used to guide precise micro-injections of various tracers in VMpo. A prior report (Craig and Zhang, 2006) described retrograde tracing results, which confirmed the selective lamina I input to VMpo and the antero-posterior (head to foot) topography. The present report describes the results of micro-injections of anterograde tracers placed at different levels in VMpo, based on the antero-posterior topographic organization of selectively nociceptive units and clusters over nearly the entire extent of VMpo. Each injection produced dense, patchy terminal labeling in a single coherent field within a distinct granular cortical area centered in the fundus of the superior limiting sulcus. The terminations were distributed with a consistent antero-posterior topography over the posterior half of the superior limiting sulcus. These observations demonstrate a specific VMpo projection area in dorsal posterior insular cortex that provides the basis for a somatotopic representation of selectively nociceptive lamina I spinothalamic activity. These results also identify the VMpo terminal area as the posterior half of interoceptive cortex; the anterior half receives input from the vagal-responsive and gustatory neurons in the basal part of the ventral medial nucleus (VMb).

Keywords

lamina I; spinothalamic; pain; thermosensory; homeostasis

INTRODUCTION

Lamina I neurons at the margin of the spinal / trigeminal superficial dorsal horn are crucial for pain and temperature sensations in primates. Modality-selective thermoreceptive and nociceptive lamina I neurons (Christensen and Perl, 1970; Craig, 2003b; Willis et al., 1974) contribute approximately half of the ascending spinothalamic fibers in monkeys and humans (Kuru, 1949, Willis et al., 1979). The advent of anterograde tracing methods using a plant

Correspondence to: Dr. A. D. Craig, Atkinson Research Laboratory, Barrow Neurological Institute, 350 West Thomas Rd., Phoenix, AZ 85013, Tel.: (602)-406-3385, FAX: (602)-406-4121, Bud.Craig@DignityHealth.org.

lectin (*Phaseolus vulgaris* leuco-agglutinin, PHA-L; Gerfen + Sawchenko, 1984) and label-conjugated dextrans (Schmued et al., 1990) provided the high resolution and sensitivity needed to identify the projections of small-diameter lamina I fibers at spinal, brainstem and thalamic levels in cat and monkey (Craig, 1993, 1995, 2003a, 2004a).

Anterograde tracing experiments in long-tailed macaque monkeys using these novel tracers revealed that a cytoarchitectonically distinct structure in posterolateral thalamus receives trigemino- and spino-thalamic lamina I terminations that are somatotopically organized along an antero-posterior gradient (head to foot; Craig et al., 1994; Craig, 2004a). It was named the posterior part of the ventral medial nucleus (VMpo), because together with the contiguous basal part of the ventral medial nucleus (VMb), it constitutes a topographically coherent structure that receives ascending input representative of all interoceptive (homeostatic sensory) activity (Beckstead et al., 1980; Pritchard et al., 2000). The lamina I terminations in VMpo consist of dense clusters of large boutons that are glutamatergic (Blomqvist et al., 1996) and form triadic synaptic complexes characteristic of thalamic relay nuclei (Beggs et al., 2003). Thus, microelectrode recordings that revealed clusters of thermoreceptive-specific (COOL) and nociceptive-specific (NS) neurons in VMpo that are topographically organized with the same antero-posterior gradient (head to foot) naturally suggested that VMpo could serve as a specific relay nucleus for pain and temperature sensations (Craig et al., 1994). This conclusion was supported by evidence that a greatly enlarged putative homologue is present in the human posterolateral thalamus (Craig et al., 1994; Blomqvist et al., 2000) at the appropriate location to match other relevant findings (Mehler, 1966; Hassler, 1970; Mesulam, 1979; Dostrovsky et al., 1992; Lenz et al., 1993; Davis et al., 1999).

Preliminary anterograde tracing evidence that VMpo projects to the fundus of the superior limiting sulcus (SLS) of the posterior insula in monkey (Craig, 1995a, 1995b, 2000; Craig et al., 1995a) was convincingly corroborated by our quantitative positron emission tomography (PET) study of graded innocuous cooling sensation in humans (Craig et al., 2000). The apparent topographic continuity of the VMpo projection with the projections of vagal-responsive and gustatory neurons in VMb to the anterior half of the fundus of the SLS (Pritchard et al., 1986; Ito and Craig, 2008a) led to the realization that this entire cortical area can serve as “interoceptive cortex” (Craig, 2002), a concept which converges with considerable clinical interests (e.g., Goldman et al., 2010; Herbert and Pollatos, 2012), and which led to fundamental ideas on the role of interoception and insular cortex in emotional awareness, in subjective time perception, and in a wide variety of other domains that drew a considerable portion of my time and attention (Craig, 2005, 2009a,b, 2010a,b, 2011). Consequently, the detailed evidence on the characteristics and the thalamo-cortical projections of VMpo neurons in the macaque that was described in meeting reports and book chapters (cited above) remained unpublished, and in the absence of detailed documentation, several authors questioned these findings (Wall, 1995; Willis et al., 2001, 2002; Graziano and Jones, 2004).

The present report is the first of a series of articles that will document in detail the physiological characteristics and the cortical projections of VMpo and neighboring sites in posterolateral thalamus of the long-tailed macaque monkey. The results described here

validate the physiological localization of VMpo and document the antero-posterior (head to foot) topographic gradient of selectively nociceptive neurons in VMpo. Its main projection to the cytoarchitectonically distinct area centered at the fundus of the SLS is shown, and the topographic organization of VMpo terminations in this area is demonstrated. This cortical area has mistakenly been included in the second somatosensory field in atlases. In the accompanying description of the architectonic organization of insular cortex in the macaque (Evrard et al., xxxx), we identify this as a distinct area and call it the posterior dorsal fundus of the insula, or Idfp. Some of these data were illustrated in preliminary reports (Craig, 1995a,b, 2000; Craig et al., 1995a).

MATERIALS AND METHODS

The material presented in this report was obtained from 15 adolescent or adult long-tailed (cynomolgus) macaque monkeys (*Macaca fascicularis*), of either sex and weighing 2.0–5.0 kg; these cases were selected from a series of 103 experiments performed over a period of almost 20 years (as explained below). The animals were treated according to the guidelines of the American Physiological Society and the NIH, and according to protocols approved by the Institutional Animal Care and Use Committee of the Barrow Neurological Institute.

Each animal was tranquilized with ketamine (25 mg i.m.) and then anesthetized with pentobarbital administered through an angiocath placed in the right saphenous vein (40 mg/kg, with supplements given as needed to maintain areflexia). Dexamethasone (10 mg) was administered; prophylactic broad-spectrum antibiotics were used in survival cases. Each animal was mounted in a stereotaxic frame, and a hole in the right or left calvarium was made aseptically. The dura was excised, and extracellular recordings were made with a tungsten-in-glass microelectrode (tip ~20 um, plated with platinum black, impedance ~200 KOhm).

Physiological localization of VMpo

Based on the histological location of VMpo (Craig, 2004a), the following strategy was designed for locating it using microelectrode recordings; (1) obtain recordings from clusters of units with large spikes responsive to low-threshold cutaneous (mechanoreceptive) or deep (proprioceptive) stimulation of the contralateral body in the main somatosensory nuclei, the ventral posterior medial (VPM; face representation) and ventral posterior lateral (VPL; arm, leg and body representation) nuclei, aiming first at the representation of the medial digits of the hand at AP +7.0, ML +8.0.; (2) make successive penetrations progressively further medial and posterior in steps of 0.25 or more, guided by the well-defined classical maps of somatosensory thalamus (macaque monkey: Mountcastle and Henneman, 1952; raccoon: Welker et al., 1964; cat: Rose and Mountcastle, 1952), in order to obtain recordings sequentially from the mechanoreceptive representations of the ear, cheek, nose, lips, and finally contralateral and ipsilateral intraoral surfaces (Bombardieri et al., 1975; Jones et al., 1986); (3) in the first penetration in which no such low-threshold responses are obtained at the same depths (taking care to note the intervening presence of CM most medially), use appropriate search stimuli that could be expected to activate neurons that receive a dense, selective input from lamina I spinothalamic neurons, viz. innocuous cool, pinch, noxious

heat, deep pressure and noxious cold (in order of increasing potential trauma), beginning most anteriorly with stimulation of the face (VMpo; as shown previously in Fig. 1 of Craig et al., 1994, and Fig. 1 of Craig and Zhang, 2006). In the following, “clusters” are multi-unit recordings selectively activated by a single stimulus modality from a common RF or closely overlapping RFs, and "background activity" refers to acoustic hash that was interpreted to signify activation of neuropil within 200 μm of the microelectrode tip.

The manual search stimuli used were based on experience gained in prior electrophysiological experiments in which lamina I spinothalamic neurons were functionally characterized in cats (e.g., Craig and Kniffki, 1985; Craig and Dostrovsky, 1991; Craig and Hunsley, 1991; Craig and Serrano, 1994; Craig et al., 2001), and also from lamina I recordings made in monkeys in order to guide the precise placement of anterograde tracer injections (Craig, 1993, 1995, 2004a). It was important to use search stimuli that were just adequate for driving lamina I neurons, because excessive noxious stimulation can quickly cause sensitization, resulting in multireceptive responses, and eventually can cause nociceptive lamina I neurons and VMpo neurons to become almost completely silent in a barbiturate-anesthetized cat or monkey. A crucial advantage was the use of platinum-plated tungsten-in-glass microelectrodes custom-built in this laboratory (Craig et al., 2001), because an excellent microelectrode, appropriately shaped and plated, can provide not only clear recordings of clusters and isolated single units in VMpo, but also background signals that, with good-quality audio equipment, can enable a discriminating ear to hear recorded activity from neighboring sources (clusters of cells and incoming afferent fibers) in the surrounding neuropil. Brief pinch stimuli were regularly applied to densely innervated regions, such as the lips, nares, eyebrow, ear, hand, shoulder, hip and foot, and audible background activity often revealed that responsive neurons were very near at that depth. Such background activation provided invaluable guidance which supported the identification of selectively nociceptive neurons with a small RF (receptive field) in an obscure location, such as the lateral chest (see **Results**, case m154, AP 6.1, ML 7.2).

Cool and cold were applied with a small plastic beaker filled with crushed ice (cooling-sensitive units almost always responded immediately, or even prior to contact; the beaker was never applied longer than 30 sec), pinch was applied with a flat 6” anatomical forceps (thermoneutral), warmth and heat were applied with a radiant heat lamp (made with a standard 150W projector bulb) from appropriate distances (noxious threshold after approximately 5 sec; Craig et al., 2001), and deep pressure was applied using fingers, fingernails and an anatomical forceps with 1 cm wide flat plates affixed to each side (Mense, 1985). Analog records were preserved on tape and on a PC computer using the program Spike2 (CED, Cambridge, UK).

Anatomical tracer injections

Nearly all experiments were survival experiments, in which injections of neuroanatomical tracers were made at selected sites by withdrawing the microelectrode and replacing it with a micropipette. Because systematic recordings and injections in VMpo were nearly impossible due to its small size (as explained in **Results**), micro-injections of different neuroanatomical tracers were made according to the particular recordings that were

serendipitously obtained in each animal. Eventually, a thorough coverage and an adequate number of cases in which the micro-injection was appropriately placed could be expected, based on the natural variation in the shape and size of VMpo and the variation in microelectrode and micro-injection placement. In general, each case was processed completely before the next injection procedure, in order to identify and address any unexpected problems.

The injection micropipette (tip ca. 15 μm) was filled with cholera toxin subunit b (CTb; 1%, List Biological, Campbell, CA, or Sigma, St. Louis, MO) or one of several conjugated dextrans (10K dextran conjugated with biotin, rhodamine, fluorescein, Alexa 546, Alexa 594, or Alexa 488; 10% in 0.01M phosphate buffer [PB], Molecular Probes / Invitrogen, Palo Alto, CA). Stereotaxic calibration was performed by aligning the micropipette with a mark on the edge of excised bone using a dissection microscope; re-alignment accuracy was estimated as better than +/− 100 μm in each dimension, based on visual inspection and recordings made with a different microelectrode in prior penetrations. In addition, care was taken to ensure that the external contour of the micro-pipette matched the contour of the microelectrode; if it did not, then as it traveled through 25 mm of brain tissue to reach VMpo, it compressed the tissue differently, and the tracks simply did not align. Iontophoretic injections were made by passing 2–7 μA pulsed positive current (5s on, 5s off) for 10–40 min. Pressure injections were made by applying pneumatic pressure pulses (Picopump, WPI, Sarasota, FL) repeatedly until a calibrated amount had been delivered, as measured using an eyepiece reticle on a dissection microscope. (In order to maximize the utilization of animals, multiple anterograde tracer injections using different tracers were generally made, sometimes on both sides of the brain, to study thalamo-cortical connections.)

The animals survived 2–4 wks, and then were tranquilized with ketamine and deeply anesthetized with pentobarbital. Intravenous heparin was administered (10000 IU), a lethal dose of pentobarbital (60 mg/kg iv) was administered, and 90 sec later the animals were perfused transcardially with 1 liter warm heparinized phosphate-buffered saline (0.1M PBS, 0.9% NaCl, 10000 IU heparin, pH 7.4, 37°C), followed by fixation with 1 liter 4% paraformaldehyde and 0.2% picric acid in PB at room temperature, and then 1.5 liter cold (10°C) 4% paraformaldehyde and 0.05% glutaraldehyde containing 10% sucrose in PB.

Histological processing

The brainstem was removed from the diencephalon by a transverse cut at the ponto-mesencephalic boundary, and the spinal cord was separated from the brainstem at the C1–2 junction. Tissue blocks were stored in 30% sucrose in PB at 4°C for 3–30 days. Serial 50 μm frozen sections (sometimes at other thicknesses, e.g., 60 μm) were cut in the coronal plane from the diencephalon and cortex and collected in Tris-buffered saline (0.1M TBS, 0.9% NaCl, pH 7.4); alternate sections were stained with thionin for injection site localization. In some cases, the thalamus was separated from the cortex and processed separately. The brainstem and spinal cord were processed as described earlier, if necessary (Craig and Zhang, 2006).

If need be, the sections were processed immunohistochemically for visualization of CTb with the ABC/DAB protocol at room temperature on a shaker table, as described before (Craig et al., 2002). Our protocol is as follows: using ample rinsing between steps in TBS and TBS-T (with 0.1% Triton-X and 0.1% NaN3), the sections are treated with: 0.02% NaIO4, 15 min; 0.1% NaBH4, 15 min; 0.5% egg white, 30 min; 2% normal horse serum (NHS), 2 hr; rabbit anti-CTb (1:40,000, List) in 2% NHS, 40–48 hr; biotinylated goat anti-rabbit IgG (1:800, Vector), 4–8 hr; ABC solution (Vector) 1 hr; and lastly, a DAB reaction (0.025% diaminobenzidine and 0.02% hydrogen peroxide for 3–7 min). The sections were mounted from TBS onto gelatin-dipped slides, air-dried, rinsed in alcohol/chloroform (30 min) and Citrisolv (a non-toxic substitute for xylene, Fisher), and coverslipped with Permount (Sigma). Fluorescent labeling was examined as soon as possible, since in some cases the fluorescent tracer labeling faded within hours after coverslipping. Fluorescent-labeled material was stored in a refrigerator (4°C) until analysis was complete.

Sections containing biotin-conjugated dextran (BDA) were simply incubated with the ABC solution followed by a DAB reaction, and sections containing fluorescent tracers were mounted, cleared and coverslipped, as described before (e.g., Ito and Craig, 2008b). Labeling was documented by two or more observers in many cases. Injection sites were plotted on individual camera lucida drawings at 14X, photographed, and re-plotted on a standard cytoarchitectonic chart of the thalamus based on one case (m18; Craig, 2004). Cytoarchitectonic delineations of the thalamus were made according to Craig (2004), using Stepniewska et al. (2003) for additional guidance. The VMpo was identified according to the cytoarchitectural criteria documented in the detailed report of anterograde labeling from lamina I (Craig, 2004a). Labeling in cortex was plotted on camera lucida drawings and then re-plotted on a standard cytoarchitectonic chart based on serial levels shown in the macaque atlas of Szabo and Cowan (1984). Color photomicrographs were made using push-processed Fujicolor 400, and digital photographic images were obtained with a Leaf Microlumina scanner (3380×2253 pixels), a Hamamatsu Orca-HR CCD camera (4000×2624 pixels), or a Nikon DS-Fi1 color CCD camera (2560×1920 pixels) and printed from Adobe Photoshop after contrast enhancement and sharpening. Histological processing and analysis of each case lasted approximately 4–6 weeks.

The quantitative estimates of micro-injection site locations shown in Table 1 are based on the ordinal value of the section containing the injection site in relation to the total number of coronal sections in which VMpo is visible in each brain. For example, if VMpo is visible on 10 consecutive thionin-stained sections (whether 1-in-2 or 1-in-4) and the micro-injection site was located on the 9th section (counting from posterior to anterior), then it was located at the level that is 90% of the length of the nucleus. The quantitative estimates of the antero-posterior location of the anterogradely labeled terminal field in Idfp for each case were calculated similarly, that is, on the basis of the ordinal numbers of the sections containing the terminal labeling field in relation to the total number of sections between the posterior limit of the SLS, where it joins the inferior limiting sulcus to become the lateral sulcus, and the limen insulae, the first section in which the frontal lobe is separate from the temporal lobe. If there are 100 sections between the posterior end of the SLS and the limen insulae, and the terminal labeling is on sections 50–60 of that set (counting from posterior to anterior), then the labeling is at levels 50–60%.

RESULTS

The 15 experiments presented in this report were selected from 74 survival and 29 acute recording experiments performed in the years 1991–2006, in which 208 isolated single units, 187 small units (i.e., not cleanly isolated), and 680 clusters were recorded in VMpo. Most of the remaining experiments provide evidence regarding modality-selective details of VMpo's projections or the characteristics and projections of neighboring regions in posterolateral thalamus, which are currently being analysed.

The long series of experiments was deemed necessary, because systematic recordings and accurately placed tracer micro-injections in VMpo could not be achieved with present technology, for several reasons: (1) VMpo is a small and structurally variable nucleus that is difficult to find with a microelectrode; (2) functional identification of selectively nociceptive neurons with small RFs located anywhere on the contralateral body is not trivial; (3) microelectrode penetrations at the required 0.25 mm intervals are difficult to reconstruct histologically, due to inevitable swelling and tissue distortion. Most importantly, as documented below, (4) precise placement of tracer micro-injections in posterolateral thalamus using a separate micro-pipette is unreliable. A double-barreled micro-electrode / micro-pipette constructed in this laboratory was inadequate for recording from single units or clusters in VMpo, though it provided satisfactory recordings of vagal-evoked potentials (Ito and Craig, 2008b).

Thus, goals were set, but in each experiment injections were placed according to the recordings that were serendipitously obtained, and the results were categorized according to the eventual, histologically verified location of the recordings and the injections. The scope of the project naturally grew to include several neighboring portions of posterolateral thalamus. As expected, the variation in microelectrode and micro-injection placement eventually provided a sufficient number of cases in which nearly the entire extent of VMpo had been sampled and in which the micro-injections were appropriately placed. The variation in the size of VMpo was considerable, and it clearly varied with the source of the monkeys; its entire antero-posterior extent was generally in the range 1.0–1.4 mm, but in some monkeys it was only 0.6 mm long, and in a few it was very difficult to identify VMpo anatomically (particularly in batches from China).

In the following, three early cases are described that validate the physiological localization of VMpo and document the unreliability of micro-injection placement. Next, the antero-posterior (head to foot) topographic gradient of selectively nociceptive neurons in VMpo is demonstrated with the results from five cases in which recordings were obtained from units and clusters with RFs distributed from head to foot, and in which the histological reconstruction showed that nearly the entire antero-posterior extent of VMpo had been sampled. Next, a single case with a large injection centered in VMpo is presented, which shows the main cortical projection of VMpo to area Idfp and ancillary projections. Finally, six cases are presented in which tracer micro-injections were made at different antero-posterior levels in VMpo; together, these cases document the antero-posterior topography of the main VMpo projection to the dorsal posterior insula.

Localization of VMpo recording sites as targets for tracer micro-injections

Figure 1 presents histological evidence from two experiments. The photomicrograph of a thionin-stained section shown in the top panel documents histologically the recordings from VMpo neurons in monkey m30. The sequence of recordings was as follows. The recordings on penetration #9 disclosed no further clusters of large spikes responsive to low-threshold mechanoreceptors, rather only background activity was heard in response to tapping the teeth. Somewhat deeper in the same penetration, background activation was heard in response to innocuous cooling applied to the contralateral lips and tongue. At that same depth in a new penetration (#10) made just 0.25 mm further posterior, small units were recorded that responded only to innocuous cooling applied to the contralateral tip of the tongue. Deeper in the penetration, units that responded only to pinch and noxious heat applied to small RFs on the lips were identified. In a new penetration made 0.25 mm further posterior, beginning at that depth and extending over a vertical distance of almost 1 mm, several single units and clusters were recorded that responded selectively to pinch applied to small RFs on the nose, cheek, or maxillary face. The final recording penetration was made another 0.25 mm further posterior, and at the same depths single units and small clusters were recorded that responded selectively to pinch applied to the hand (digits 1–3; response shown at bottom left of Fig. 1), anterior lower arm, and dorsal ear (at successively deeper sites). The microelectrode was then used to make a penetration 2 mm lateral to that final recording penetration, and a marking lesion was electrically burned (5 μA, 20 sec) at the depth corresponding to the middle of the dorso-ventral range of nociceptive recordings in the final penetration. The microelectrode was then replaced with a micropipette, which was inserted to the same depth at an antero-posterior position between the last two recording penetrations, where an iontophoretic injection of the tracer CTb (2 μA, 17 min) was made.

The photomicrograph in the top panel of Figure 1 shows the thionin-stained section which best displays the marking lesion burned with the microelectrode (indicated by the long arrow on the right) and the histological trace of the CTb injection micro-pipette. The lesion lies at the same depth as the micro-injection of CTb (indicated by the long arrow on the left), as intended. That depth lies within the cytoarchitectonic limits of VMpo, which are denoted by the large triangular arrowheads. That localization verifies that the single units and clusters that were recorded with thermoreceptive- and nociceptive-specific responses were in fact obtained from VMpo neurons.

However, the photomicrograph also shows that the CTb micro-pipette did not penetrate in exact alignment with the recording microelectrode. The injection was located at the intended depth and very close to the intended medio-lateral position, but it was almost 200 μm too posterior.

The photomicrograph in the lower panel of Figure 1 shows the histological verification of VMpo recordings made during an acute experiment (vm1). In this monkey, dye-marked penetrations were used to align the histological plane of section as closely as possible with the direction of the recording microelectrode penetrations, and serial thalamic sections were stained with thionin. The weakly gliotic histological traces of three recording penetrations through VMpo are visible in the section displayed in the lower panel of Figure 1. Single units and clusters of units that were recorded over a vertical extent > 1 mm during these

penetrations evinced responses selectively to pinch and/or noxious heat and/or deep noxious pressure applied within small RFs on the ear or the hand. Marking lesions were made at the dorsal and ventral borders of this physiologically-defined region in the most medial penetration of the three shown in Figure 1; as can be seen, these lesions lie on the dorsal and ventral boundaries of the histologically visible VMpo, which is delimited by the large triangular arrowheads. Thus, the recordings were again identified as VMpo units. (An image of these lesions and quantitative records from this case were shown in the original report [Craig et al., 1994.])

Figure 2 presents histological evidence from another experiment (m36) demonstrating different issues with the placement of anterograde tracer injections in VMpo. The photomicrograph in the top panel shows the histological traces of two recording penetrations; in the lateral penetration (#7), a series of single units and clusters selectively responsive to pinch applied to the ear, eyelid and lips were recorded, and in the medial penetration (#8), a similar series of nociceptive responses was preceded by recordings from single units selectively responsive to innocuous cooling applied to the lips. The photomicrograph in the lower panel shows the histological trace of the final penetration (#9) in the next consecutive (alternate) thionin section; this penetration was made 0.25 mm posterior to penetrations #7 and #8, and single units and clusters were recorded that were selectively responsive to pinch and/or noxious heat applied to the medial hand and fingers D1–2. Following the recordings, a micro-pipette was inserted in order to make an iontophoretic injection of Gdx (FITC-labeled dextran) at the site of the units responsive to pinch on the face in penetration #7, and a second micro-pipette was used to make an injection of Rdx (TRITC-labeled dextran) at the site of units responsive to pinching the hand in penetration #9.

The histological trace of the micro-pipette used to make the Gdx injection is visible in the upper panel; it followed the track of penetration #7 closely, as intended. However, that injection failed; for some unknown reason, almost no fluorescent tracer was deposited.

The histological trace of the micro-pipette used to make the Rdx injection is visible in the lower panel; the inset shows the fluorescent injection site, which was centered in the next posterior adjacent (fluorescent) section. These images show that the Rdx injection was located within VMpo, however, it lies almost 0.5 mm medial to the intended target in penetration #9. Fortunately, anterogradely labeled terminations were found in the dorsal posterior insula, which provided the first evidence for the cortical projection of VMpo. Nevertheless, this case clearly showed that the accurate placement of a tracer micro-injection at an identified recording site in VMpo using a separate micro-pipette was an unreliable event.

The topographic gradient of selectively nociceptive VMpo neurons

In order to document the basic antero-posterior topography of recorded VMpo neurons, the stereotaxic coordinates of units and clusters responsive selectively to pinch (i.e., with no initial sensitivity to low-threshold mechanical stimulation) were collated from 5 experiments in which (1) responses were obtained from RFs located in all three major regions of the body: the face, head, ear and neck (region 1); hand, arm, shoulder, and chest (region 2); and

foot, leg, abdomen, rump, and tail (region 3), and in which (2) microelectrode penetrations were made through nearly the entire antero-posterior extent of VMpo. The photomicrographs in Figure 3 illustrate all of the microelectrode penetrations in two of these cases, m154 (left panels) and m57 (right panels). The penetrations in both of these cases include very posterior (upper panels) and very anterior (lower panels) levels of VMpo that were at or near (within 1–2 sections) its extreme limits. These photomicrographs can be directly compared with the 3-dimensional plots in Figures 4A and 4B, which show the distribution of recording sites with RFs in regions 1, 2 and 3 that were obtained in these two cases. These graphs document the finding that the recording sites with RFs in region 1 (face) were generally located most anteriorly, whereas the recording sites with RFs in region 3 were generally located most posteriorly, while the recording sites with RFs in region 2 were located in the middle. These plots also show the medial-to-lateral shift in the stereotaxic location of VMpo across its antero-posterior extent.

In particular, in case m154 (left panels of Figure 3, 3-dimensional graph in Figure 4A), the overall distribution of RFs in regions 1, 2, and 3 was (9, 5, 7). Recordings from VMpo units and clusters selectively responsive to pinch were obtained in microelectrode penetrations at all three antero-posterior levels (AP 6.7, 6.3, and 6.1); in each portion of VMpo, test stimuli were applied in all three regions, and in each penetration, very few units and no clusters were recorded that remained unidentified. At the most anterior level (lower left panel of Figure 3), AP 6.7, four recording sites with region 1 RFs were identified in the medial penetration (ML 5.9; upper lip, ear, lower lip, tongue; in order of increasing depth) and one in the lateral penetration (ML 6.3; lateral upper lip). At the next posterior level (middle left panel of Figure 3), AP 6.3, two recording sites in the medial penetration (ML 6.9) had RFs in region 1 (eyelid, mid cheek), and in the lateral penetration (ML 7.2) one site had an RF in region 1 (ear) and two had an RF in region 2 (lateral hand, ventral lower arm). Finally, at the most posterior level (top left panel of Figure 3), AP 6.1, one recording site in the medial penetration (ML 7.2) had an RF in region 1 (ear), two recording sites had a region 2 RF (dorsal hand, lateral chest) and three sites had a region 3 RF (lateral abdomen, posterior leg, lateral thigh), and in the lateral penetration (ML 7.5) one recording site had an RF in region 2 (lateral shoulder) and four sites had an RF in region 3 (lateral hip, lateral foot, anterior knee).

Similarly, the RFs identified in the 3-dimensional graph shown in Figure 4B correspond with the visible microelectrode penetrations through VMpo that are indicated with arrows in the photomicrographs shown in the right panels of Figure 3 for case m57. The overall distribution of RFs in m57 was (11, 7, 1). In this case, it is obvious from the histology that additional microelectrode penetrations through the lateral portions of VMpo (visible at the two more anterior levels of m57 in Fig. 3B2 and B3) would have been beneficial, but that is hindsight; it was good fortune simply to have recorded and identified VMpo units and clusters with RFs in all 3 regions in penetrations that covered nearly the entire antero-posterior extent of VMpo. As noted above, the five cases that are collated here satisfied those two criteria.

The 3-dimensional graph in Figure 4C shows the regional distribution of RFs for selectively nociceptive, pinch-responsive VMpo neurons recorded in five cases (m57, m65, m86, m154,

and m177). The total numbers of RFs in regions 1, 2, and 3 for these five cases were (38, 18, 15). These data were collated by aligning the centers of region 2 recordings in each case (that is, by superimposing the geometric means on all three axes). This graph clearly shows that region 1 RFs (head) were distributed generally in the anterior portion of VMpo, region 3 RFs (foot) were found generally in the posterior portion of VMpo, and region 2 RFs (hand) were found generally in the middle of VMpo. In other words, pinch-responsive units and clusters in VMpo display an antero-posterior somatic topography that is consistent with the antero-posterior gradient of the somatotopy that was observed both globally and at high resolution for the anterogradely labeled lamina I terminations in VMpo (Craig, 2004).

These extracellular microelectrode recordings did not reveal a fine-grained somatotopy; individual units within multi-unit clusters always displayed overlapping RFs within a moderately small region, and closely neighboring units and clusters in a single microelectrode penetration often had RFs at closely neighboring skin locations, but large jumps in RF location in a penetration were commonly observed, as these data demonstrate. The spatial resolution of these methods is sufficient to demonstrate the overall topographic gradient of VMpo, but not the organization within the individual groups of neurons in VMpo or the relationships between these groups. Nevertheless, in each animal, the same overall antero-posterior topographic gradient was consistently observed for nociceptive VMpo units. The thermoreceptive-specific (COOL) VMpo neurons were always found in the most antero-medial part of VMpo; they are not described further in the present report.

Identification of the main cortical projection of VMpo to the dorsal posterior insular cortex

Representative evidence is shown in Figures 5 and 6 from a case in which a large pressure injection (400nL) of 1% CTb was made with a micro-pipette that was directed at the site of recordings of clusters selectively responsive to pinch and heat applied to the hand (m70). The photomicrograph (Fig. 5A) and the drawing (Fig. 5B) show that the dense ‘core’ of the physiologically-guided injection (dark grey in Fig. 1B) filled nearly all of the posterior portion of VMpo and spread dorsally into SG, ventrally and laterally into the remnant of Po, and ventromedially into APT and the mesencephalon. The surrounding ‘halo’ (light gray) spread dorsally into Pla and Plm, and laterally into the posterior aspect of VPL. The injection core and halo also extended anteriorly and filled nearly the entire trigeminal portion of VMpo (not shown). As reported previously (Craig and Zhang, 2006), this large injection produced strong retrograde labeling of lamina I and other spinothalamic neurons throughout the spinal cord and medulla.

The main field of anterogradely-labeled terminations in this case occupies the fundus and nearby walls of the posterior portion of the superior limiting sulcus (SLS). As shown in Figure 5C, there is dense terminal labeling in layers 3b and 4, accompanied by terminal and retrograde labeling in layer 6; this labeling extends an equal distance (approximately 1 mm measured in layer 4) away from the center of the fundus on both the medial and lateral walls. Comparably dense labeling is present in this distinct area beginning at the posterior end of the insula (i.e., at the union of the SLS with the LS) and extending anteriorly nearly to the antero-lateral end of the central sulcus, that is, through most of the posterior half of the SLS (see Fig. 6). Figure 5C also shows sharply delimited fields of less intense labeling

that extend ventrally through the entire insular cortex at this posterior level, and the borders of these terminal labeling fields correspond well with the distinct cytoarchitectonic areas that are marked in the adjacent Nissl-stained section shown in Figure 5D. As described in detail in the accompanying report (Evrard et al., xxxx), we refer to the area centered at the fundus of the SLS in the posterior insula that receives the main projection of VMpo as the posterior portion of the dorsal fundus of the insula (Idfp). The remaining areas at this level that receive input from neighboring portions of posterolateral thalamus are the dorsal and ventral granular insular areas (Igd and Igv) and the posterior portion of the ventral fundus of the insula (Ivfp; note that the leading "I" is omitted from all labels in Fig. 5C for clarity; Evrard et al., xxxx).

Figure 6 depicts the overall distribution of terminal labeling in case m70, plotted directly onto drawings of the original sections (top), and transposed onto the series of standard coronal sections of the macaque monkey brain that was used to collate these data and make overall comparisons (bottom), which covers the entire antero-posterior extent of insular cortex (copied with permission from the atlas of Szabo and Cowan, 1984).

Successful experiments, in which cortical labeling was observed from physiologically-guided, histologically verified injections of anterograde tracers in VMpo, always contained dense terminal labeling in Idfp. The main cortical projection of VMpo matches the cytoarchitectonic demarcation of Idfp. Ancillary projections from VMpo that are not described here in detail include patches of labeling in the convex belly of the macaque insula (e.g., levels A13.4, 14.6 and 15.5 in Fig. 6; see also Fig. 5E,F), particularly in the dysgranular mound area (Idm; see companion report, Evrard et al., xxxx), the fundus of the cingulate sulcus (area 24c; not shown), and the fundus of the central sulcus (area 3a; e.g., levels A12.1 and 13.4, Fig. 6) .

The topographic gradient of the VMpo projection to the dorsal posterior insula

Anterograde labeling in the dorsal posterior insular cortex that was obtained following a single tracer micro-injection in VMpo is shown here for 6 cases. These data document the antero-posterior topographic gradient of the main VMpo projection to Idfp.

Table 1 presents the specific details of these six cases, and Figure 7 illustrates the injection site in each case. Both are organized so that the case with the most posterior injection site (m55R) is shown first and cases with progressively more anterior injection sites are shown in succession, ending with the case in which the injection was placed in the most anterior portion of VMpo (m58R). Because each brain is structurally unique and because the cutting plane always varied somewhat, it is not easy to estimate the antero-posterior level of each micro-injection in VMpo from these photomicrographs and drawings. Accordingly, a quantitative estimate of injection site location is provided in Table 1, based on the ordinal value of the section containing the injection site in relation to the total number of coronal sections in which VMpo is visible in each brain. Thus, the micro-injection of BDA in case m55R is in the third section from a total of 16, in other words, it was centered at a level approximately 3/16 or 19% of the distance between the posterior and anterior limits of VMpo. Similarly, the micro-injection of BDA in case m54R is in the ninth section of eleven overall, or at a level approximately 82% of the entire posterior to anterior extent of VMpo.

The main anterograde middle-layer terminal labeling in the cortex of each of these cases was located in the fundus and adjacent walls of the posterior SLS, that is, in Idfp. For example, photomicrographs of the labeling in Idfp in case m54R are shown in Figure 8, and the original plotted sections for that case are shown in Figure 9. Figure 8A shows darkfield images of the labeling in consecutive 1-in-5 60 μm-thick sections. Proceeding from posterior to anterior in sections with decreasing number from upper left towards lower right, the main burst of terminal labeling begins in the ventral portion of the medial wall in section 10c, occupies the entire fundus of the SLS in sections 9c through 9a, and finally wanes in the lateral wall in sections 8a and 7c. The pair of photomicrographs in Figure 8D,E show that the medio-lateral extent of the field of labeling at its center in section 9b matches the cytoarchitectonic limits of area Idfp, marked by the arrowheads. The field of labeling is essentially continuous, and there is no labeling at other levels of Idfp, yet the labeled field contains discrete patches of high density. The terminal labeling is most dense in layers 3b and 4, with more modest anterograde (and retrograde) labeling in layer 6 and in layer 3a. The supragranular labeling extends all the way to layer 1, which clearly receives weak input in some cases (Fig. 8B,C), though such labeling is not visible in all cases.

The plotted labeling illustrated in Figure 9 shows two ancillary VMpo projections in this case; small patches of dense labeling in case m54R are located in the dysgranular portion of insular cortex as well as in the fundus of the central sulcus (area 3a). The patch of terminal labeling visible in section 5c in Figure 9 is located in the dysgranular mound area Idm, similar to the discrete patches of labeling shown for case m70 in Figures 3 and 4.

Figure 10 presents a standardized comparison of the antero-posterior location of the terminal labeling in Idfp in each of these six cases, progressing from the case with the most posterior micro-injection in VMpo on the left (m55R) to the case with the most anterior micro-injection (m58R) on the right. The standard drawings of insular cortex at each antero-posterior level are taken directly from the coronal drawings of the Szabo and Cowan (1984) atlas, as indicated by the numerical labels. The standardized representations of labeling emphasize the coherence of labeling across the fundus, but also show the patchiness at the ends of each field, as can be appreciated by directly comparing the actual labeling shown for case m54R in Figure 8 with the original plots in Figure 9 and with the standardized plot in Figure 10. The curling or spiral pattern of labeling in the main VMpo projection to Idfp, progressing from the posterior medial wall to the fundus to the anterior lateral wall, that is visible in case m54R is a common pattern across the entire data set, and it occurs in four of the six cases presented in Figure 10 (cases m137R, m175R, m54R and m58R). In other cases, the patchiness of the labeling in Idfp is more pronounced, often appearing only on one wall or the other with a sharp border at the center of the fundus (e.g., case m120R in Fig. 10) or occupying the central fundus without extending further into the nearby walls (e.g., case m55R in Fig. 10). Nevertheless, the plots in Figure 10 indicate that a single coherent field of anterograde labeling was present at a particular antero-posterior level in Idfp in all six of the illustrated cases, consistent with the presence of a single coherent somatotopic map in VMpo. These plots show that the terminal labeling in Idfp was found at progressively more anterior locations in Idfp as the tracer micro-injection site was placed at successively more anterior locations in VMpo, moving from left to right in Figure 10. Thus, the antero-posterior topographic gradient of VMpo is maintained in its main projection to dorsal

posterior insular cortex, and it provides the basis for a similarly coherent somatotopic map in Idfp, with head anterior and foot posterior.

A different representation of the same antero-posterior gradient is presented in Table 1. The quantitative estimate of the antero-posterior location of each micro-injection in VMpo, as presented in column four and described above, can be compared directly to the quantitative estimate of the antero-posterior location of the anterogradely labeled terminal field in Idfp for each case, which is provided in the right-most two columns of Table 1. These show the location of the center of the terminal field (column 5) and its longitudinal extent (column 6) for each case on the basis of the ordinal numbers of the sections containing the labeling in relation to the total number of sections between the posterior limit of the SLS (i.e., the junction with the inferior limiting sulcus and the lateral sulcus) and the limen insulae (a morphologically distinct point marked by the separation from the temporal lobe). These values clearly show that as the location of the micro-injection in VMpo shifted further towards the anterior end of VMpo, so too the location of the field of terminal labeling in Idfp shifted further towards the anterior end of insular cortex, thus documenting again the antero-posterior (head to foot) topographic gradient of the VMpo projection to Idfp.

The VMpo projection to the fundus of the SLS occupies approximately the posterior half of its entire extent. The SLS extends approximately 2–3 mm further anterior than the limen insulae, and thus approximately the anterior half of the overall extent of the SLS, or area Idfa, remains unlabeled; the homeostatic afferent input that ascends via the VMb nucleus is represented in that region (Pritchard et al., 2000; Ito and Craig, 2008a).

DISCUSSION

The present report provides detailed documentation on the topographic organization of VMpo and its main cortical projection to the fundus of the posterior half of the SLS in the long-tailed (cynomolgus) macaque monkey. A topographic (head to foot) gradient of selectively nociceptive clusters and units was demonstrated over the antero-posterior extent of VMpo. That matches the gradient of the somatotopically organized lamina I spinothalamic terminations in VMpo (Craig, 2004) and of lamina I neurons retrogradely labeled following micro-injections of the tracer CTb in VMpo (Craig and Zhang, 2006). Precise micro-injections of anterograde tracers in VMpo reliably produced a single coherent field of dense, patchy terminal labeling in the cytoarchitectonically distinct granular area centered in the fundus of the posterior SLS; we refer to this area as the posterior dorsal fundus of insular cortex (Idfp), as described in the companion report (Evrard et al., xxxx). The location of the VMpo termination field in Idfp shifted along an antero-posterior gradient consonant with the antero-posterior location of the injection site in VMpo. These data indicate that a somatotopic representation of selectively nociceptive lamina I spinothalamic activity exists in area Idfp of the macaque monkey that is organized along an antero-posterior (head to foot) topographic gradient. Together with prior findings and the comparative evidence discussed below, these results identify this VMpo projection field as the posterior half of interoceptive cortex, and indicate that a homologous interoceptive representation is present in humans.

Comparison with prior anatomical and physiological findings in posterolateral thalamus of the macaque

Soon after the first descriptions of PHA-L-labeled lamina I trigemino- and spinothalamic terminations in the macaque monkey (Craig, 1990, 1991, 1992), my colleagues and I published a short report announcing the discovery of the cytoarchitectonically distinct, antero-posteriorly somatotopic lamina I trigemino- and spino-thalamo-cortical relay nucleus VMpo in monkey and human, based on double-label anterograde tracing, microelectrode recordings, cytoarchitectonic analyses, retrograde labeling and immunohistochemical staining (Craig et al., 1994). Our report built upon the first descriptions of dense spinothalamic terminations in posterolateral thalamus of the macaque monkey by Boivie (1979) and by Berkeley (1980). Dense spinothalamic terminations in the “posterior / supragenicular (Po-SG) region” were ascribed to ascending lamina I axons also by Ralston and Ralston (1992), though they did not perceive a cytoarchitectonically distinct nucleus or a topographic organization, probably because they conflated it with VPI. The detailed description of the cytoarchitectonic characteristics of VMpo and the somatotopic organization of PHA-L-labeled and anterogradely double-labeled terminations in the macaque monkey was published a few years later (Craig, 2004a). The present observations are consistent with those findings.

The article that has been cited as the first report of nociceptive-specific neurons in posterolateral thalamus of macaque monkeys states that the units had bilateral, often whole body RFs, and the investigators concluded the responses were likely due to neuronal irritation by the microelectrode (Perl and Whitlock, 1961). Some thirty years later, a study in squirrel monkeys reported that only 8 of 21 units in the posterior region were “nociresponsive”, while 23 of 46 units in VPI were, of which 10 were nociceptive-specific (Apkarian and Shi, 1994). Most of the nociceptive-specific units in VPI had trigeminal RFs. Those were likely VMpo neurons, because VPI receives no trigeminal lamina I input (Craig et al., 1999; Craig, 2004a), and in New World monkeys it abuts anterior VMpo, as we observed in our examinations of VMpo in the owl monkey (Blomqvist et al., 1996; Craig et al., 1999).

Our antidromic activation study of lamina I spinothalamic neurons that project to VMpo in the macaque monkey revealed that thermoreceptive-specific (COOL), nociceptive-specific (NS) and polymodal nociceptive (HPC) cells all project to VMpo (Dostrovsky and Craig, 1996); these are the same three major categories of spinothalamic lamina I neurons that are found in the cat (see Craig et al., 2001; Yu et al., 2005; Zhang et al., 2006). Our study in the owl monkey documented recordings from both COOL and selectively nociceptive clusters in VMpo, and large clusters of COOL cells with RFs on the nares were identified in antero-medial VMpo at the site of dense PHA-L-labeled terminations from a specialized cluster of trigeminal COOL lamina I cells (Craig et al., 1999). These prior findings are entirely consistent with the present results, and they support the view that VMpo relays “labeled lines” that serve discriminative, modality-specific sensations of temperature and pain.

The original description of VMpo was questioned by several authors (Wall, 1995; Willis et al., 2001, 2002; Ralston, 2003; Graziano and Jones, 2004; Davidson et al., 2008). Rebuttals to all criticisms have been published with detailed anatomical analyses and positive

anatomical and physiological counter-evidence (Craig et al., 1995b; Craig and Blomqvist, 2002; Craig, 2004a,b, 2006, 2008, 2011). Independent anatomical confirmation of VMpo was included in a study of spinothalamic terminations in motor thalamus in the macaque monkey (Stepniewska et al., 2003). Strong corroboration was provided by the demonstration of dense anterograde labeling in VMpo ("Po-SG"), VPI, and the medial thalamus (ventral caudal MD) following cervical spinal injections of a viral tracer in the New World Cebus monkey (Dum et al., 2009). As the authors stated, those sites correspond precisely to the major lamina I spinothalamic termination sites that I identified with PHA-L in the macaque (Craig, 2004).

The present findings demonstrate that selectively nociceptive clusters and units in VMpo are topographically organized along an antero-posterior gradient (head to foot); the RFs in anterior VMpo were located on rostral parts of the body, and RFs in posterior VMpo were located on caudal parts of the body. This topographic gradient fits with the prior anterograde and retrograde tracing observations, and it supports the conclusion that VMpo serves as a thalamo-cortical relay nucleus for pain and temperature sensations. As noted in **Results**, however, the histological reconstructions of these extracellular microelectrode recordings had insufficient spatial resolution to determine whether a continuous, fine-grained somatotopic representation is present, and disjunctive shifts in RF location in a single penetration were almost always observed. A coherent somatotopic organization seems likely, because: (1) systematic RF shifts in successive units and clusters were often observed in single microelectrode penetrations (e.g., down the arm, or across the face); and, (2) a single, coherent field of anterogradely labeled terminations was observed in Idfp in every case. Nevertheless, the topographic organization in VMpo clearly differs from the fine-grained lemniscal somatotopy in the much larger somatosensory thalamic nuclei (VPM and VPL), in both precision and magnification factor. The structural anchors and the trophic patterns underlying the 3-dimensional organization of VMpo neurons remain to be determined.

Comparison with prior findings in posterior insular cortex of the macaque

Microelectrode recordings from sparse, antero-posteriorly topographic nociceptive-specific neurons in the fundus of the SLS of the barbiturate-anesthetized macaque monkey were first reported at a meeting by Dostrovsky and Craig (1996; documented in Fig. 1 of Craig, 2010). Laser-evoked potentials (LEPs) were recorded from the scalp of macaque monkeys anesthetized with Saffan (alfaxolone/alfadolone) by Baumgärtner et al. (2006), and they showed convincing evidence of an antero-posterior (head to foot) topographic gradient. The 3-dimensional source reconstructions (based on a pediatric human model) indicated a somatotopically organized current source in the dorsal posterior insular cortex, consistent with the present results. Later, Huang and Craig (2007, 2008) reported at meetings their use of an intracortical multi-electrode array to identify the focus of antero-posteriorly organized LEPs in the fundus of the SLS in Saffan-anesthetized macaque monkeys. They showed with retrograde labeling from the insular cortical LEP focus that the thalamic origin of the cortical LEP they had identified was VMpo neurons at the precise location where a focal LEP from the same stimulation site was recorded with a shorter latency.

Anterograde transneuronal viral labeling in the New World Cebus monkey was reported in the dorsal posterior ("granular") insula, the dorsal bank of the lateral sulcus, and the fundus of the cingulate sulcus by Dum et al. (2009), which they attributed to ascending lamina I terminations in VMpo ("Po-SG"), VPI, and ventral caudal MD, respectively, as noted above. Their findings are consistent with the PHA-L-labeled lamina I terminations (Craig, 2004a) and with thalamo-cortical labeling data in this laboratory, except that the labeled patches they illustrated in the dorsal posterior insula were not centered in the fundus of the SLS. This discrepancy could be due to the fact that they labeled only a portion of the entire VMpo projection field; it could also reflect selectivity in the transneuronal viral labeling technique (see Discussion in Evrard and Craig, 2008). By contrast, the present data reveal the entire extent of the topographically organized VMpo projection field in Idfp. The present data also reveal ancillary VMpo projections to dysgranular insular cortex, the fundus of the central sulcus, and the fundus of the cingulate sulcus.

Prior neuroanatomical investigations of somatosensory areas in the lateral sulcus and parietal operculum recognized a border on the medial wall of the SLS approximately 0.5–1.0 mm from the center of the fundus, consistent with the medial limit of Idfp indicated by VMpo terminations in the present study (Roberts and Akert, 1963; Jones and Burton, 1976; Friedman et al., 1980; Mesulam and Mufson, 1982). However, our architectonic study of insular cortex is the first to delimit area Idfp (Evrard et al., xxxx); prior investigators included the fundus of the posterior SLS in the second somatosensory area (S2), based on recording studies that were interpreted to indicate a mixed antero-posterior (head-to-foot) and medio-lateral somatotopy, and also on tracing studies that showed interconnections with somatosensory areas in thalamus and cortex (Burton and Jones, 1976; Robinson and Burton 1980; Friedman et al., 1980). Those recording studies were later re-interpreted in support of a double representation organized from lateral to medial (face to foot) somatotopically (Whitsel et al., 1969; Burton et al., 1995; Krubitzer et al., 1995), which modern studies confirmed in humans (Eickhoff et al., 2006b, 2007). But, the early tracing studies that produced labeling in the fundus of the monkey SLS that was interpreted as S2 have yet to be explained. This neuroanatomical confusion needs to be clarified, because in monkey and human atlases the fundus of the SLS is labeled as S2.

The present findings provide a precise anatomical explanation for those tracing results. For example, tracer injections in the portions of S1 that represent face, hand and foot in one study produced well-delimited, antero-posteriorly topographic labeling in the fundus of the SLS, separate from patches of labeling in the operculum (see cases CM63R, CM74 and CM75 in Figs. 7, 8, and 11 of Friedman et al., 1980). The injection sites in S1 in each case included the fundus of the central sulcus, and since that region (i.e., area 3a) is topographically interconnected with VMpo, according to tracing material in this laboratory, it is likely topographically interconnected with Idfp as well (see also Whitsel et al., 2009). In fact, labeling in the posterolateral thalamus was illustrated for one of those prior cases just posterior to VPM, at the location of anterior VMpo, consistent with this explanation (see levels 230, 260 in Fig. 7, case CM74; Friedman et al., 1980). In another study, a tracer injection interpreted as "posterior VPM" in the thalamus produced well-delimited, dense labeling in the fundus of the posterior SLS (see Fig. 6, case RM17R in Burton and Jones, 1976), which was interpreted as the face representation of S2. But, modern evidence

indicates that the face representation of the S2 areas actually lies at the lateral edge of the operculum, almost 20 mm away. The illustrated tracer injection in that case was centered in the region between VPI and VMb at the posterior end of VPM, at the same location just described in the study of Friedman et al. (1980). However, that region was identified as the anterior-most portion of VMpo by anterogradely labeled trigemino-thalamic lamina I terminations, and it was carefully documented with photomicrographs, because these prior studies had mis-interpreted it as VPM (see Fig. 13 in Craig, 2004a). This explanation is confirmed by the fact that the labeling in the fundus of the SLS in cases CM74 and RM17R of the prior studies lies at the topographically appropriate level for projections from the most anterior part of VMpo, according to the results displayed in the present report (i.e., near the antero-lateral end of the central sulcus, similar to case m58R in Figure 10 of this report).

Thus, area Idfp, the distinct area centered at the fundus of the posterior half of the SLS, is NOT part of the second somatosensory areas. It is the main terminal projection field of the lamina I spino-thalamo-cortical relay nucleus VMpo. It contains the primary cortical representations of the discriminative sensations of cool, warm, sharpness, pricking pain and burning pain. Further, it is the posterior half of interoceptive cortex, as I discuss later.

The lamina I spinothalamic pathway includes three major response categories, COOL, NS, and HPC, and all three types of neurons project to VMpo. Each of these physiological types of lamina I spinothalamic cells is associated with a distinct feeling from the body that can be localized well in humans. That certainly suggests that a distinct somatotopic map for each response category exists within Idfp, that is, that each “labeled line” terminates in its own somatotopically organized cortical map. The present observations show that "selectively nociceptive" VMpo neurons are topographically organized antero-posteriorly over nearly the entire extent of VMpo. Both NS-like and HPC-like neurons are included in the set of "selectively nociceptive" VMpo neurons. In the present data, each anterograde tracer injection in VMpo produced a single coherent termination field in Idfp, which must contain the projections of both NS-like and HPC-like VMpo neurons. If there are separate maps, they could form parallel strips, as suggested by the sharp border at the center of the fundus of the SLS in particular cases, such as m120R and m58R (see Fig. 10); alternatively, they could be intertwined, as suggested by the curling (spiral or helical) pattern of labeling in several cases, such as m137R, m175R, and m54R, as well as by certain functional imaging data in humans (see below; Brooks et al., 2005; Henderson et al., 2011). The present findings do not resolve this question, although they do indicate that the primary sensory cortex for nociception is located in Idfp. The present anterograde tracing data do not distinguish any physiological categories; they show that projections from the entire extent of VMpo to Idfp are antero-posteriorly topographic. Thus, since the thermoreceptive-specific COOL lamina I spinothalamic neurons are represented in the most antero-medial portion of VMpo, then the tracing data described in the present study strongly suggest that they project to the most antero-medial portion of Idfp. Physiological evidence identifying these three classes in VMpo, histological documentation of their distributions within VMpo, and anterograde tracing evidence of their terminations in Idfp are currently being analysed and will be described later.

Finally, a “ventral somatosensory” field (VS) has been suggested to exist in the depths of the LS or the SLS lateral to S2/PV, in the neighborhood of the VMpo terminus in area Idfp, but its identity is unclear. The characteristics of VS have been reported as follows: low-threshold responses in the lower bank of the LS with a well-defined lateral-to-medial somatotopy in owl monkeys (Cusick et al., 1989); low-threshold responses in the lower bank of the LS in one long-tailed macaque, but in posterior insula in another, with no apparent topography (Krubitzer et al., 1995); low-threshold responses in posterior insula and the lower bank of the LS, with a lateral-to-medial gradient in one marmoset monkey, but an anterior-to-posterior gradient in another (Qi et al., 2002); and, mostly high-threshold or deep somatic responses in posterior insula with “variable” topography in titi monkeys, interpreted to indicate a rostral and a caudal VS (Coq et al., 2004). Some of those recordings may have originated from sensitized nociceptive neurons in Idfp, but it seems likely that recordings were made in one or more different areas in the upper and lower banks of the LS and the granular face of the posterior insula that receive somatosensory, thermosensory, nociceptive, auditory, and/or vestibular inputs, which remain to be identified. The thalamo-cortical labeling data in this laboratory support that possibility.

Comparison with relevant anatomical and physiological evidence in posterolateral thalamus of humans

Dense small-fiber spinothalamic terminations in posterolateral thalamus were identified by R. Hassler using silver-stained fiber degeneration after an anterolateral cordotomy in a baboon; he called that region “ventrocaudalis portae” (V.c.po.), or the gateway (portal) to the main somatosensory nucleus and related it directly to pain (Hassler and Riechert, 1959, Hassler, 1960, 1970). At about the same time, Mehler (1966) described a dense, small-fiber termination field in a cytoarchitectonically distinct region posterior and inferior to the main somatosensory nucleus in one human anterolateral cordotomy patient, which he called “the ventral caudal portion of the ventrocaudalis nucleus”; his report was later confirmed by Mesulam (1979). We identified that region of the human posterolateral thalamus as VMpo, based on cytoarchitectonic and immunohistochemical analyses indicating a structural homology with VMpo of the macaque (Blomqvist et al., 2000). It is enormously enlarged with respect to the macaque VMpo, as it is also in the common chimpanzee, the bonobo, and the gorilla (Craig et al., 2007). The name “ventrocaudalis portae” suitably describes its histological appearance in humans and great apes, because it visibly enwraps the lemniscal and spinothalamic fibers entering posterolateral thalamus (see Figs. 1B, 6B and 7B in Blomqvist et al., 2000; Craig et al., 2007); however, that name inappropriately associates it with the main somatosensory nucleus, which relays mechanoreceptive and proprioceptive activity, that is, exteroceptive activity.

Micro-stimulation in that region, posterior and inferior to the main somatosensory nucleus, can produce reports of well-localized pricking or burning pain sensations in awake human patients, in stark contrast to reports of tingling or buzzing voiced upon stimulation in the main somatosensory thalamus. Hassler originally associated stimulation-evoked pain with the “ventrocaudalis portae” (Hassler and Riechert, 1959, Hassler, 1960, 1970), but later he focused on the “ventrocaudalis parvicellularis” (V.c.pc.), which is equivalent to the monkey’s VPI. Stimulation-evoked pain was also reported by Halliday and Logue (1972),

Tasker (1984), Dostrovsky et al. (1992, 2000), Lenz et al. (1993), and Davis et al. (1995, 1996, 1999). Consistent with the present findings, nociceptive-specific units were recorded in the same region (Dostrovsky et al., 1992, 2000; Lenz & Dougherty 1997; Davis et al., 1996). Cool sensations were also elicited by stimulation in this region. Davis et al. (1999) recorded cooling-sensitive thermoreceptive-specific units at the same sites from which they elicited reports of cool sensations with micro-stimulation, and they reconstructed those sites to the same region that we identified anatomically as the human VMpo (Blomqvist et al., 2000).

Attempts to identify VMpo in human thalamus based on magnetic resonance images of infarcts that produced thermanesthesia and central (thalamic) pain in single patients were unsuccessful (Montes et al., 2005; Kim et al., 2007; Krause et al., 2012), until a rigorous mathematical alignment method was used to merge the images from a group of 10 patients (Sprenger et al., 2012). That study identified the epi-center of such lesions at MNI (x,y,z) coordinates (−14, −23, 0 or 1), which matches the center of the area we identified histologically as the human VMpo, in their notation (−13.75, −22.25, 0). Our description of that location was a range of values (“A −0.5 to +2.0, L 12.0 to 16.0, H −1.0 to +1.0”) that must be averaged. It must be corrected by AP-23.0 mm, since we measured distance from the posterior commissure, as the anterior commissure was not visible in our sections (Craig et al., 1994; Blomqvist et al., 2000), and the AC-PC distance in the standard template Colin27 used by Sprenger et al. (2012) is 23.0 mm.

Comparison with relevant evidence in posterior insular cortex of humans

Our PET study of discriminative thermal sensation showed that the only site in contralateral cortex with activation that was linearly correlated with the innocuous cool stimulus temperatures was centered in the fundus of the SLS in human posterior insular cortex (Craig et al., 2000). Lamina I neurons provide the only ascending pathway that conveys a linear representation of innocuous cool stimulus temperatures (Craig et al., 1994, 2001; Dostrovsky and Craig, 1996; Craig, 2004a); thus, our PET data provided convincing evidence that the projection target of thermoreceptive-specific VMpo neurons in human cortex matches the VMpo projection to Idfp identified by our tracing data, which are documented in the present report. Subsequent functional magnetic resonance imaging (fMRI) studies corroborated the location of human thermosensory (cooling) cortex (Maihofner et al., 2002; Hua et al., 2005), and electroencephalographic (EEG) analyses suggested a comparable location for warm activation (Iannetti et al., 2003; Stancak et al., 2006). In addition, we showed an antero-posterior topographic gradient in the dorsal posterior insula for innocuous cool stimulation in humans, consistent with the gradient identified by the present findings (Hua et al., 2005).These results strongly imply that the cortical projection target of nociceptive VMpo neurons in humans is also located in the fundus of the posterior SLS and has an antero-posterior topography.

Specific nociceptive activation in the dorsal posterior insular cortex recognized to indicate a potential primary nociceptive cortical sensory area was reported for these sub-modalities of painful stimuli (in chronological order): noxious heat, Brooks et al. (2002); C-fiber LEP, Kakigi et al. (2003); noxious esophageal distension, Strigo et al. (2003); intramuscular

hypertonic saline injection (muscle pain), Kupers et al. (2004); graded noxious heat, Keltner et al. (2006); and, pinprick, Baumgartner et al. (2010). The assertion that this region contains primary nociceptive cortex is supported also by the attention-related enhancement of activity when subjects perform a nociceptive discrimination task (Schlereth et al., 2003) and by the findings that this region is a source of the earliest cortical LEP and that its magnitude correlates with stimulus strength and perceived pain intensity (Iannetti et al., 2005).

Studies in humans indicating that nociceptive activation in the dorsal posterior insular cortex is somatotopically organized along an antero-posterior (head to foot) gradient include these sub-modalities of painful stimuli: LEPs, Vogel et al. (2003); noxious heat, Brooks et al. (2005), Baumgartner et al. (2010); both intracutaneous and intramuscular hypertonic saline injection, Henderson et al. (2007, 2011); and, pinprick, Baumgartner et al. (2010). This gradient is distinct (orthogonal) from the lateral to medial (head to foot) gradient of non-specific activation in the neighboring opercular somatosensory areas (S2/PV, or OP1/OP4 in human). These studies in human are clearly consistent with the antero-posterior topographic gradient of VMpo terminations in Idfp demonstrated in the present report, and they fulfill the prediction made by the present results. These data strongly support the conclusion that the dorsal posterior insula of humans contains a VMpo terminus that is homologous with the VMpo projection field in Idfp documented by the present evidence in the macaque monkey.

Corroborative evidence in humans is also provided by clinical studies in which intracerebral depth electrodes were used for electrical stimulation in human epilepsy patients. A recently published summary of one team's experience over 12 years states definitively that dorsal posterior insular cortex is the only region of cortex in which stimulation can reproducibly evoke reports of localized contralateral pain sensations in awake humans (Mazzola et al., 2012). The authors concluded that activation of a distributed network must be involved, rather than a specific sensory cortical representation, because pain was evoked in only 10% of stimulation trials in the insula. However, Figure 3 of their report shows data that fit with the present findings. That figure shows the location of every stimulation site in a subgroup of patients, plotted as distance from the dorsal posterior pole of the insula, and colored to show whether stimulation at that site produced a pain sensation or not. The graph indicates very clearly that stimulation produced a pain report at 100% (15/15) of sites within 2 cm of the dorsal posterior pole, at 53% (10/19) of sites between 2 and 3 cm distant, at 22% (6/27) of sites between 3 and 4 cm distant, and at 0% (0/15) of sites beyond. To my mind, those findings support the conclusion that primary nociceptive sensory cortex is located in the dorsal posterior insular cortex of humans, consistent with the present experimental results in monkeys.

This conclusion is also supported by reports that a lesion of this same region of cortex can cause localized contralateral loss or dysfunction of pain and temperature sensibilities in humans (Schmahmann and Liefer, 1992; Greenspan et al., 1999; Birklein et al., 2005). In contrast, large lesions of S1 and S2 do not reduce pain sensation, unless they involve area 3a (see Perl, 1984; Vierck et al., 2013) or the dorsal posterior insula (see discussion of Ploner et al., 1999, in Craig and Blomqvist, 2002; Craig, 2003b). The clinical effects of lesions can vary, though, due to various factors that cannot be controlled in inhomogeneous samples (e.g., compensatory plasticity, undetected damage, ipsilateral pathways; see Olausson et al.,

2001; Voets et al., 2006), which might explain two contradictory reports (Starr et al., 2009; Veldhuijzen et al., 2010).

Recent anatomical studies of the operculo-insular region of human cortex medial to S2/PV (OP1/OP4) identified two cytoarchitectonically distinct granular areas, OP2 and OP3, which occupy the fundus of the SLS at the posterior pole of insular cortex, where the SLS merges with the inferior limiting sucus (ILS) and becomes the LS (Eickhoff et al., 2006a; Kurth et al., 2010). The more posterior area OP2, which extends into the LS, was identified as primary vestibular cortex (Eickhoff et al., 2006c). In macaques, primary vestibular cortex is the retroinsular area (Ri) in the fundus of the LS (Chen et al., 2010), which is adjoined anteriorly by area Idfp in the fundus of the SLS. Thus, if the human equivalent of Ri is OP2, then the human equivalent of Idfp could be OP3. The human area OP3 was suggested to correspond to VS of primates (Eickhoff et al., 2007); however, as noted above, area VS in monkeys remains to be defined. The granular area OP3 defined anatomically in the fundus of the SLS in human cortex, just anterior to the primary vestibular cortex in OP2, seems appropriately positioned to correspond with the functional imaging evidence cited above and with area Idfp in the macaque monkey. Future studies can test this hypothesis. Another possibility is that area OP3 in human is homologous with the combined areas Idfp and Idfa in monkey (i.e., interoceptive cortex); if not, then there should be another granular area in the fundus of the SLS anterior to OP3 that will correspond with the vagal-responsive and gustatory area Idfa of the macaque.

Area Idfp is the posterior half of interoceptive cortex

Lamina I neurons were formerly regarded as "pain and temperature" neurons. However, lamina I neurons receive input from small-diameter afferents that relate the mechanical, thermal, metabolic and vascular status of skin, muscle, joint, and visceral tissue compartments; that is, lamina I neurons receive homeostatic afferent input that represents the physiological condition of all tissues of the body that are sympathetically innervated. The spinal and brainstem projections of lamina I neurons validate this conclusion (Craig, 1993, 1995). The ascending lamina I spinothalamic pathway is an interoceptive pathway, which in humans provides the basis for affective feelings from the body and the sense of the "material me" (Craig, 2002).

In addition to the discriminative sensations of temperature and pain, the ascending lamina I pathway to VMpo and dorsal posterior insula includes other physiological categories that generate distinct, affective feelings from the body in humans, such as itch, muscle ache/burn, warm, and C-tactile (“slow brush”) affective touch. Little comparative physiological evidence related to these categories is available (see Andrew and Craig, 2001; Wilson et al., 2002), but functional imaging evidence in humans indicates that these feelings are represented in dorsal posterior insular cortex. Specific activation of dorsal posterior insular cortex was reported for dynamic and passive cycling (Williamson et al., 1997), graded histamine-induced itch (Drzezga et al., 2001), and C-tactile affective touch (Olausson et al., 2002). In addition, an antero-posterior topographic gradient in the dorsal posterior insula was convincingly demonstrated for C-tactile affective touch in single subjects using multivariate analysis (Bjornsdotter et al., 2009). All of these sensations can at least roughly be

localized on the body. Thus, in concert with the present results and the findings discussed above, these observations suggest that the dorsal posterior insular cortex contains somatotopic representations of these, and perhaps all, affective feelings from the body. The dorsal posterior insula in humans does not contain simply the primary thermosensory and nociceptive representations.

The lamina I pathway to VMpo and Idfp is complemented by the solitary nucleus pathway to VMb and Idfa, which like the lamina I pathway is phylogenetically unique to primates (Beckstead et al., 1980; Pritchard et al., 1986, 2000; Carmichael and Price, 1996; Ito and Craig, 2008a). The combined structure VMpo+VMb provides a complete representation of homeostatic afferents, that is, the sensory complements of both the spinal (sympathetic; VMpo) and the cranial (parasympathetic; VMb) divisions of the autonomic nervous system. Areas Idfp and Idfa in the macaque monkey together form a continuous strip over the entire length of the fundus of the SLS, which constitutes interoceptive cortex (Craig, 2002; Evrard et al., xxxx). Similarly, in humans, vagal and gustatory stimuli activate the region in dorsal mid/posterior insula just anterior to the region activated by noxious and thermal stimuli (e.g., Henderson et al., 2003; Veldhuizen et al., 2011; Wang et al., 2008), consistent with the presence of a coherent interoceptive representation of all homeostatic afferent activity.

The present findings directly support this concept by demonstrating that area Idfp contains a topographic representation of ascending lamina I activity. Area Idfp is the posterior half of interoceptive cortex. Prior to the observations described in this and the companion article (Evrard et al., xxxx), the posterior fundus of the SLS has been regarded as part of S2, and the anterior fundus either as gustatory cortex or as a premotor area. By recognizing the continuity of the discrete granular area centered at the fundus of the SLS over its entire length, and by demonstrating the complete, topographically continuous representation of homeostatic afferent input in Idfp+Idfa by way of VMpo+VMb, our observations establish the neuroanatomical foundation for the concept of interoceptive cortex.

Conclusions

These data document the topographic organization of selectively nociceptive neurons in the macaque monkey's VMpo, and they demonstrate the topographically organized projection of VMpo neurons to Idfp, the distinct granular area centered at the fundus of the SLS in dorsal posterior insular cortex. These findings predict the presence of an antero-posteriorly somatotopic primary nociceptive sensory cortex in area Idfp in monkey, and similarly in area OP3 in humans. This prediction is strongly supported already by the studies in human cited above.

The organization of representations of all distinct affective feelings in dorsal posterior insular cortex remains to be shown, including in particular the putative distinct representations of NS (first, pricking pain) and HPC (second, burning pain) activity. The primary nociceptive sensory cortex in dorsal posterior insula is part of interoceptive cortex, a larger area that represents the homeostatic afferent input from all tissues of the entire body, from both sympathetically (lamina I, VMpo) and parasympathetically (solitary nucleus, VMb) innervated tissues and organs. I have suggested that interoceptive cortex serves as the tensile anchor for the formation of the operculated insula in anthropoid primates (Craig,

2011; see Discussion in Evrard et al., xxxx), and as the basis for the homeostatic integration that underlies the role of anterior insular cortex in such distinctly human domains as music, time perception and subjective awareness (Craig, 2009, 2010a). The future identification of distinct, topographically-organized modules within interoceptive cortex and the insula of monkeys and humans, using functional imaging, *in vivo* optical imaging and molecular genetic architectonic markers, could provide crucial insights into the proposals that homeostatic valuation guides emotional behavior and that a fundamental neural construct for an interoceptive feeling from the body ultimately engenders any subjective feeling in humans (Craig, 2009, 2010a; Seth et al., 2011; Fitzgerald et al., 2012).

Acknowledgments

The author is especially grateful to Drs. Anders Blomqvist, Henry Evrard, and Irina Strigo for comments on the manuscript. Sincere gratitude is expressed to the following colleagues and friends who shared the experience of one or more of these experiments: Drs. M.C. Bushnell, Y. DeKoninck, J.O. Dostrovsky, P. Dougherty, A. C. Ericsson, H. Evrard, J. Huang, S.-I. Ito, K. Krout, R.H. LaMotte, B. Lumb, and E. Rausell. These individuals deserve gratitude and recognition for providing excellent technical support: M. Auldridge, L. Brady, T. Fleming, M. Marcogliese, and M. Tatum.

Grant support: NIH grants NS25616 and NS41287, the Barrow Neurological Foundation and the James S. McDonnell Foundation.

LITERATURE CITED

Adreani CM, Kaufman MP. Effect of arterial occlusion on responses of group III and IV afferents to dynamic exercise. J Appl Physiol. 1998; 84:1827–1833. [PubMed: 9609773]

Andrew D, Craig AD. Spinothalamic lamina I neurons selectively sensitive to histamine: a central neural pathway for itch. Nat Neurosci. 2001; 4(1):72–77. [PubMed: 11135647]

Apkarian AV, Bushnell MC, Treede RD, Zubieta JK. Human brain mechanisms of pain perception and regulation in health and disease. Eur J Pain. 2005; 9:463–484. [PubMed: 15979027]

Banzett RB, Mulnier HE, Murphy K, Rosen SD, Wise RJ, Adams L. Breathlessness in humans activates insular cortex. NeuroReport. 2000; 11(10):2117–2120. [PubMed: 10923655]

Baumgärtner U, Tiede W, Treede RD, Craig AD. Laser-evoked potentials are graded and somatotopically organized anteroposteriorly in the operculoinsular cortex of anesthetized monkeys. J Neurophysiol. 2006; 96(5):2802–2808. [PubMed: 16899640]

Baumgärtner U, Iannetti GD, Zambreanu L, Stoeter P, Treede RD, Tracey I. Multiple somatotopic representations of heat and mechanical pain in the operculo-insular cortex: a high-resolution fMRI study. J Neurophysiol. 2010; 104(5):2863–2872. [PubMed: 20739597]

Beckstead RM, Morse JR, Norgren R. The nucleus of the solitary tract in the monkey: projections to the thalamus and brain stem nuclei. J Comp Neurol. 1980; 190:259–282. [PubMed: 6769981]

Beggs J, Jordan S, Ericson AC, Blomqvist A, Craig AD. Synaptology of trigemino- and spinothalamic lamina I terminations in the posterior ventral medial nucleus of the macaque. J Comp Neurol. 2003; 459(4):334–354. [PubMed: 12687703]

Benison AM, Chumachenko S, Harrison JA, Maier SF, Falci SP, Watkins LR, Barth DS. Caudal granular insular cortex is sufficient and necessary for the long-term maintenance of allodynic behavior in the rat attributable to mononeuropathy. J Neurosci. 2011; 31(17):6317–6328. [PubMed: 21525272]

Berkley KJ. Spatial relationships between the terminations of somatic sensory and motor pathways in the rostral brainstem of cats and monkeys. I. Ascending somatic sensory inputs to lateral diencephalon. J Comp Neurol. 1980; 193:283–317. [PubMed: 7430431]

Birklein F, Rolke R, Müller-Forell W. Isolated insular infarction eliminates contralateral cold, cold pain, and pinprick perception. Neurology. 2005; 65(9):1381. [PubMed: 16275823]

Bjornsdotter M, Loken L, Olausson H, Vallbo A, Wessberg J. Somatotopic organization of gentle touch processing in the posterior insular cortex. J Neurosci. 2009; 29(29):9314–9320. [PubMed: 19625521]

Blomqvist A, Ericson AC, Craig AD, Broman J. Evidence for glutamate as a neurotransmitter in spinothalamic tract terminals in the posterior region of owl monkeys. Exp Brain Res. 1996; 108:33–44. [PubMed: 8721153]

Blomqvist A, Zhang ET, Craig AD. Cytoarchitectonic and immunohistochemical characterization of a specific pain and temperature relay, the posterior portion of the ventral medial nucleus, in the human thalamus. Brain. 2000; 123:601–619. [PubMed: 10686182]

Boivie J. An anatomical reinvestigation of the termination of the spinothalamic tract in the monkey. J Comp Neurol. 1979; 186:343–370. [PubMed: 110850]

Bombardieri RA Jr, Johnson JI Jr, Campos GB. Species differences in mechanosensory projections from the mouth to the ventrobasal thalamus. J Comp Neurol. 1975; 163:41–63. [PubMed: 1159110]

Brooks JC, Nurmikko TJ, Bimson WE, Singh KD, Roberts N. fMRI of Thermal Pain: Effects of Stimulus Laterality and Attention. Neuroimage. 2002; 15(2):293–301. [PubMed: 11798266]

Brooks JC, Zambreanu L, Godinez A, Craig AD, Tracey I. Somatotopic organisation of the human insula to painful heat studied with high resolution functional imaging. Neuroimage. 2005; 27(1): 201–209. [PubMed: 15921935]

Burton H, Jones EG. The posterior thalamic region and its cortical projection in new world and old world monkeys. J Comp Neurol. 1976; 168:249–302. [PubMed: 821975]

Burton H, Craig AD Jr, Poulos DA, Molt J. Efferent projections from temperature sensitive recording loci within the marginal zone of the nucleus caudalis of the spinal trigeminal complex in the cat. J Comp Neurol. 1979; 183:753–788. [PubMed: 762271]

Burton H, Fabri M, Alloway K. Cortical areas within the lateral sulcus connected to cutaneous representations in areas 3b and 1: A revised interpretation of the second somatosensory area in macaque monkeys. J Comp Neurol. 1995; 355:539–562. [PubMed: 7636030]

Carmichael ST, Price JL. Sensory and premotor connections of the orbital and medial prefrontal cortex of macaque monkeys. J Comp Neurol. 1995; 363:642–664. [PubMed: 8847422]

Chen A, DeAngelis GC, Angelaki DE. Macaque parieto-insular vestibular cortex: responses to self-motion and optic flow. J Neurosci. 2010; 30(8):3022–3042. [PubMed: 20181599]

Christensen BN, Perl ER. Spinal neurons specifically excited by noxious or thermal stimuli: marginal zone of the dorsal horn. J Neurophysiol. 1970; 33:293–307. [PubMed: 5415075]

Coq JO, Qi H, Collins CE, Kaas JH. Anatomical and functional organization of somatosensory areas of the lateral fissure of the New World titi monkey (Callicebus moloch). J Comp Neurol. 2004; 476(4):363–387. [PubMed: 15282711]

Craig AD, Burton H. Spinal and medullary lamina I projection to nucleus submedius in medial thalamus: a possible pain center. J Neurophysiol. 1981; 45:443–466. [PubMed: 6783739]

Craig AD, Kniffki K-D. Spinothalamic lumbosacral lamina I cells responsive to skin and muscle stimulation in the cat. J Physiol (Lond). 1985; 365:197–221. [PubMed: 4032311]

Craig AD. Lamina I trigeminothalamic projections in the monkey. Soc Neuosci Abstr. 1990; 16:1144.

Craig AD, Hunsley SJ. Morphine enhances the activity of thermoreceptive cold-specific lamina I spinothalamic neurons in the cat. Brain Res. 1991; 558:93–97. [PubMed: 1933385]

Craig AD, Dostrovsky JO. Thermoreceptive lamina I trigeminothalamic neurons project to the nucleus submedius in the cat. Exp Brain Res. 1991; 85:470–474. [PubMed: 1716595]

Craig AD. Lamina I trigeminothalamic and spinothalamic terminations in the monkey. Amer. Pain Soc. Abstr. 1991; 10:48.

Craig AD. Organization of lamina I terminations in the posterior thalamus of the cynomolgus monkey. Soc Neurosci Abstr. 1992; 18:385.

Craig AD, Bushnell MC, Zhang E-T, Blomqvist A. A thalamic nucleus specific for pain and temperature sensation. Nature. 1994; 372:770–703. [PubMed: 7695716]

Craig AD, Serrano LP. Effects of systemic morphine on lamina I spinothalamic tract neurons in the cat. Brain Res. 1994; 636:233–244. [PubMed: 8012807]

Craig, AD. Supraspinal projections of lamina I neurons. In: Besson, J-M.; Guilbaud, GOH., editors. Forebrain Areas Involved in Pain Processing. Paris: John Libbey; 1995. p. 13-26.

Craig AD, Krout K, Zhang E-T. Cortical projections of VMpo, a specific pain and temperature relay in primate thalamus. Soc Neurosci Abstr. 1995a; 21:1165.

Craig AD, Zhang ET, Bushnell MC, Blomqvist A. Pain in the brain and lower parts of the anatomy - Reply. Pain. 1995b; 62:391–393.

Craig AD, Zhang ET, Blomqvist A. A distinct thermoreceptive subregion of lamina I in nucleus caudalis of the owl monkey. J Comp Neurol. 1999; 404:221–234. [PubMed: 9934996]

Craig AD, Chen K, Bandy D, Reiman EM. Thermosensory activation of insular cortex. Nat Neurosci. 2000; 3:184–190. [PubMed: 10649575]

Craig, AD. The functional anatomy of lamina I and its role in post-stroke central pain. In: Sandkühler, J.; Bromm, B.; Gebhart, GF., editors. Nervous System Plasticity and Chronic Pain. Amsterdam: Elsevier; 2000. p. 137-151.

Craig AD, Krout K, Andrew D. Quantitative response characteristics of thermoreceptive and nociceptive lamina I spinothalamic neurons in the cat. J Neurophysiol. 2001; 86:1459–1480. [PubMed: 11535691]

Craig AD. How do you feel? Interoception: the sense of the physiological condition of the body. Nat Rev Neurosci. 2002; 3(8):655–666. [PubMed: 12154366]

Craig AD, Blomqvist A. Is there a specific lamina I spinothalamocortical pathway for pain and temperature sensations in primates? J Pain. 2002; 3:95–101. [PubMed: 14622793]

Craig AD. Distribution of trigeminothalamic and spinothalamic lamina I terminations in the cat. Somatosens Mot Res. 2003a; 20(3–4):209–222. [PubMed: 14675960]

Craig AD. Pain mechanisms: labeled lines versus convergence in central processing. Annu Rev Neurosci. 2003b; 26:1–30. [PubMed: 12651967]

Craig AD. Distribution of trigeminothalamic and spinothalamic lamina I terminations in the macaque monkey. J Comp Neurol. 2004a; 477(2):119–148. [PubMed: 15300785]

Craig AD. Lamina I, but not lamina V, spinothalamic neurons exhibit responses that correspond with burning pain. J Neurophysiol. 2004b; 92(4):2604–2609. [PubMed: 15163673]

Craig AD. Forebrain emotional asymmetry: a neuroanatomical basis? Trends Cogn Sci. 2005; 9(12): 566–571. [PubMed: 16275155]

Craig AD, Zhang ET. Retrograde analyses of spinothalamic projections in the macaque monkey: input to posterolateral thalamus. J Comp Neurol. 2006; 499(6):953–964. %20. [PubMed: 17072831]

Craig AD. Retrograde analyses of spinothalamic projections in the macaque monkey: input to ventral posterior nuclei. J Comp Neurol. 2006; 499(6):965–978. %20. [PubMed: 17072832]

Craig AD. Retrograde analyses of spinothalamic projections in the macaque monkey: input to the ventral lateral nucleus. J Comp Neurol. 2008; 508(2):315–328. [PubMed: 18322921]

Craig AD. How do you feel - now? The anterior insula and human awareness. Nat Rev Neurosci. 2009; 10:59–70. [PubMed: 19096369]

Craig AD. Emotional moments across time: a possible neural basis for time perception in the anterior insula. Philos Trans R Soc Lond B Biol Sci. 2009; 364(1525):1933–1942. [PubMed: 19487195]

Craig AD. The sentient self. Brain Struct Funct. 2010a; 214(5–6):563–577. [PubMed: 20512381]

Craig AD. Once an island, now the focus of attention. Brain Struct Funct. 2010b; 214(5–6):395–396. [PubMed: 20512362]

Craig AD. Significance of the insula for the evolution of human awareness of feelings from the body. Ann N Y Acad Sci. 2011; 1225:72–82. [PubMed: 21534994]

Cusick CG, Wall JT, Felleman DJ, Kaas JH. Somatotopic organization of the lateral sulcus of owl monkeys: Area 3b, S-II, and a ventral somatosensory area. J Comp Neurol. 1989; 282:169–190. [PubMed: 2496153]

Davidson S, Zhang X, Khasabov SG, Simone DA, Giesler GJ Jr. Termination zones of functionally characterized spinothalamic tract neurons within the primate posterior thalamus. J Neurophysiol. 2008; 100(4):2026–2037. [PubMed: 18701750]

Davis KD, Tasker RR, Kiss ZHT, Hutchison WD, Dostrovsky JO. Visceral pain evoked by thalamic microstimulation in humans. NeuroReport. 1995; 6:369–374. [PubMed: 7756631]

Davis KD, Kiss ZHT, Tasker RR, Dostrovsky JO. Thalamic stimulation-evoked sensations in chronic pain patients and in nonpain (movement disorder) patients. J Neurophysiol. 1996; 75:1026–1037. [PubMed: 8867115]

Davis KD, Lozano AM, Manduch M, Tasker RR, Kiss ZHT, Dostrovsky JO. Thalamic relay site for cold perception in humans. J Neurophysiol. 1999; 81:1970–1973. [PubMed: 10200232]

Del Parigi A, Chen K, Salbe AD, Gautier JF, Ravussin E, Reiman EM, Tataranni PA. Tasting a liquid meal after a prolonged fast is associated with preferential activation of the left hemisphere. NeuroReport. 2002; 13:1141–1145. [PubMed: 12151757]

Derbyshire SWG, Jones AKP. Cerebral responses to a continual tonic pain stimulus measured using positron emission tomography. Pain. 1998; 76:127–135. [PubMed: 9696465]

Disbrow E, Roberts T, Krubitzer L. Somatotopic organization of cortical fields in the lateral sulcus of Homo sapiens: evidence for SII and PV. J Comp Neurol. 2000; 418(1):1–21. [PubMed: 10701752]

Dostrovsky, JO.; Wells, FEB.; Tasker, RR. Pain sensations evoked by stimulation in human thalamus. In: Inoka, R.; Shigenaga, Y.; Tohyama, M., editors. Processing and Inhibition of Nociceptive Information, International Congress Series 989. Amsterdam: Excerpta Medica; 1992. p. 115-120.

Dostrovsky JO, Craig AD. Cooling-specific spinothalamic neurons in the monkey. J Neurophysiol. 1996; 76(6):3656–3665. [PubMed: 8985864]

Dostrovsky JO, Craig AD. Nociceptive neurons in primate insular cortex. Soc Neurosci Abstr. 1996; 22:111.

Dostrovsky, JO. Role of thalamus in pain. In: Sandkühler, J.; Bromm, B.; Gebhart, GF., editors. Nervous System Plasticity and Chronic Pain. Amsterdam: Elsevier; 2000. p. 245-258.

Dostrovsky, JO.; Manduch, M.; Davis, KD.; Tasker, RR.; Lozano, AM. Thalamic stimulation-evoked pain and temperature sites in pain and non-pain patients. In: Devor, M.; Rowbotham, MC.; Wiesenfeld-Hallin, Z., editors. Proceedings of the 9th World Congress on Pain. IASP Press; 2000. p. 419-425.

Drzezga A, Darsow U, Treede R, Siebner H, Frisch M, Munz F, Weilke F, Ring J, Schwaiger M, Bartenstein P. Central activation by histamine-induced itch: analogies to pain processing: a correlational analysis of O-15 H(2)O positron emission tomography studies. Pain. 2001; 92(1–2): 295–305. [PubMed: 11323151]

Dum RP, Levinthal DJ, Strick PL. The spinothalamic system targets motor and sensory areas in the cerebral cortex of monkeys. J Neurosci. 2009; 29(45):14223–14235. [PubMed: 19906970]

Eickhoff SB, Schleicher A, Zilles K, Amunts K. The human parietal operculum. I. Cytoarchitectonic mapping of subdivisions. Cereb Cortex. 2006a; 16(2):254–267. [PubMed: 15888607]

Eickhoff SB, Amunts K, Mohlberg H, Zilles K. The human parietal operculum. II. Stereotaxic maps and correlation with functional imaging results. Cereb Cortex. 2006b; 16(2):268–279. [PubMed: 15888606]

Eickhoff SB, Weiss PH, Amunts K, Fink GR, Zilles K. Identifying human parieto-insular vestibular cortex using fMRI and cytoarchitectonic mapping. Hum Brain Mapp. 2006c; 27(7):611–621. [PubMed: 16281284]

Eickhoff SB, Grefkes C, Zilles K, Fink GR. The somatotopic organization of cytoarchitectonic areas on the human parietal operculum. Cereb Cortex. 2007; 17(8):1800–1811. [PubMed: 17032710]

Ettlin DA, Zhang H, Lutz K, Järmann T, Meier D, Gallo LM, Jäncke L, Palla S. Cortical activation resulting from painless vibrotactile dental stimulation measured by functional magnetic resonance imaging (fMRI). J Dent Res. 2004; 83(10):757–761. [PubMed: 15381714]

Evrard HC, Craig AD. Retrograde analysis of the cerebellar projections to the posteroventral part of the ventral lateral thalamic nucleus in the macaque monkey. J Comp Neurol. 2008; 508(2):286–314. [PubMed: 18322920]

Fitzgerald TH, Friston KJ, Dolan RJ. Action-specific value signals in reward-related regions of the human brain. J Neurosci. 2012; 32(46):16417–16423. [PubMed: 23152624]

Friedman DP, Jones EG, Burton H. Representation pattern in the second somatic sensory area of the monkey cerebral cortex. J Comp Neurol. 1980; 192(1):21–41. [PubMed: 7410612]

Frot M, Mauguiere F. Dual representation of pain in the operculo-insular cortex in humans. Brain. 2003; 126(Pt 2):438–450. [PubMed: 12538410]

Gauriau C, Bernard JF. Posterior triangular thalamic neurons convey nociceptive messages to the secondary somatosensory and insular cortices in the rat. J Neurosci. 2004; 24(3):752–761. [PubMed: 14736861]

Gerfen CR, Sawchenko PE. An anterograde neuroanatomical tracing method that shows the detailed morphology of neurons, their axons and terminals: Immunohistochemical localization of an axonally transported plant lectin, Phaseolus vulgaris leucoagglutinin (PHA-L). Brain Res. 1984; 290:219–238. [PubMed: 6198041]

Graziano A, Jones EG. Widespread thalamic terminations of fibers arising in the superficial medullary dorsal horn of monkeys and their relation to calbindin immunoreactivity. J Neurosci. 2004; 24(1): 248–256. [PubMed: 14715957]

Greenspan JD, Lee RR, Lenz FA. Pain sensitivity alterations as a function of lesion location in the parasylvian cortex. Pain. 1999; 81:273–282. [PubMed: 10431714]

Halliday, AM.; Logue, V. Painful sensations evoked by electrical stimulation in the thalamus. In: Somjen, GG., editor. Neurophysiology Studied in Man. Amsterdam: Excerpts Medica; 1972. p. 221-230.

Hassler R, Riechert T. Klinische und anatomische Befunde bei stereotaktischen Schmerzoperationen im thalamus. Arch Psychiatr. 1959; 200:93–122.

Hassler R. Die zentralen Systeme des Schmerzes. Acta Neurochirurgica. 1960; 8:353–423. [PubMed: 13712178]

Hassler, R. Dichotomy of facial pain conduction in the diencephalon. In: Hassler, R.; Walker, AE., editors. Trigeminal Neuralgia. Philadelphia: Sanders; 1970. p. 123-138.

Heath CJ, Jones EG. An experimental study of ascending connections from the posterior group of thalamic nuclei in the cat. J Comp Neurol. 1971; 141:397–426. [PubMed: 4101677]

Henderson LA, Woo MA, Macey PM, Macey KE, Frysinger RC, Alger JR, Yan-Go F, Harper RM. Neural responses during Valsalva maneuvers in obstructive sleep apnea syndrome. J Appl Physiol. 2003; 94:1063–1074. [PubMed: 12433858]

Henderson LA, Gandevia SC, Macefield VG. Somatotopic organization of the processing of muscle and cutaneous pain in the left and right insula cortex: a single-trial fMRI study. Pain. 2007; 128(1–2):20–30. [PubMed: 17011704]

Henderson LA, Rubin TK, Macefield VG. Within-limb somatotopic representation of acute muscle pain in the human contralateral dorsal posterior insula. Hum Brain Mapp. 2011

Herbert BM, Ulbrich P, Schandry R. Interoceptive sensitivity and physical effort: implications for the self-control of physical load in everyday life. Psychophysiology. 2007; 44(2):194–202. [PubMed: 17343703]

Hilty L, Jancke L, Luechinger R, Boutellier U, Lutz K. Limitation of physical performance in a muscle fatiguing handgrip exercise is mediated by thalamo-insular activity. Hum Brain Mapp. 2011; 32(12):2151–2160. [PubMed: 21154789]

Hua LH, Strigo IA, Baxter LC, Johnson SC, Craig AD. Anteroposterior somatotopy of innocuous cooling activation focus in human dorsal posterior insular cortex. Am J Physiol Regul Integr Comp Physiol. 2005; 289(2):R319–R325. [PubMed: 15805097]

Huang J, Craig AD. Intracortical recordings of pain-related laser evoked potentials in operculoinsular cortex of the anesthetized macaque monkey. Soc Neurosci Online. 2007; 70:23.

Huang J, Craig AD. Multiple laser evoked potential sources in the neighborhood of the operculoinsular cortex of the anesthetized macaque monkey. Soc Neurosci Online. 2008; 369:23.

Iannetti GD, Truini A, Romaniello A, Galeotti F, Rizzo C, Manfredi M, Cruccu G. Evidence of a specific spinal pathway for the sense of warmth in humans. J Neurophysiol. 2003; 89(1):562–570. [PubMed: 12522202]

Iannetti GD, Zambreanu L, Cruccu G, Tracey I. Operculoinsular cortex encodes pain intensity at the earliest stages of cortical processing as indicated by amplitude of laser-evoked potentials in humans. Neuroscience. 2005; 131:199–208. [PubMed: 15680703]

Ito SI. Possible representation of somatic pain in the rat insular visceral sensory cortex: a field potential study. Neurosci Lett. 1998; 241(2–3):171–174. [PubMed: 9507948]

Ito SI, Craig AD. Thalamocortical projections of the vagus-responsive region of the basal part of the ventral medial nucleus in monkeys. Soc Neurosci Online. 2008a; 364:10.

Ito SI, Craig AD. Striatal projections of the vagal-responsive region of the thalamic parafascicular nucleus in macaque monkeys. J Comp Neurol. 2008b; 506(2):301–327. [PubMed: 18022943]

Jones EG, Powell TPS. An analysis of the posterior group of thalamic nuclei on the basis of its afferent connections. J Comp Neurol. 1971; 143:185–216. [PubMed: 5148972]

Jones EG, Burton H. Cytoarchitecture and somatic sensory connectivity of thalamic nuclei other than the ventrobasal complex in the cat. J Comp Neurol. 1974; 154:395–432. [PubMed: 4132971]

Jones EG, Burton H. Areal differences in the laminar distribution of thalamic afferents in cortical fields of the insular, parietal, and temporal regions of primates. J Comp Neurol. 1976; 168:197–248. [PubMed: 821974]

Jones, EG. The Thalamus. New York: Plenum; 1985.

Jones EG, Schwark HD, Callahan PA. Extent of the ipsilateral representation in the ventral posterior medial nucleus of the monkey thalamus. Exp Brain Res. 1986; 63:310–320. [PubMed: 3758248]

Kakigi R, Tran TD, Qiu Y, Wang X, Nguyen TB, Inui K, Watanabe S, Hoshiyama M. Cerebral responses following stimulation of unmyelinated C-fibers in humans: electro- and magneto-encephalographic study. Neurosci Res. 2003; 45:255–275. [PubMed: 12631462]

Kaufman MP, Hayes SG, Adreani CM, Pickar JG. Discharge properties of group III and IV muscle afferents. Adv Exp Med Biol. 2002; 508:25–32. [PubMed: 12171119]

Keltner JR, Furst A, Fan C, Redfern R, Inglis B, Fields HL. Isolating the modulatory effect of expectation on pain transmission: A functional magnetic resonance imaging study. J Neurosci. 2006; 26(16):4437–4443. [PubMed: 16624963]

Kerr, FWL.; Lippmann, HH. Advances in Neurology Pain. New York: Raven Press; 1974. The primate spinothalamic tract as demonstrated by anterolateral cordotomy and commissural myelotomy; p. 147-156.

Kim JH, Greenspan JD, Coghill RC, Ohara S, Lenz FA. Lesions limited to the human thalamic principal somatosensory nucleus (ventral caudal) are associated with loss of cold sensations and central pain. J Neurosci. 2007; 27(18):4995–5004. [PubMed: 17475808]

Krause T, Brunecker P, Pittl S, Taskin B, Laubisch D, Winter B, Lentza ME, Malzahn U, Villringer K, Villringer A, Jungehulsing GJ. Thalamic sensory strokes with and without pain: differences in lesion patterns in the ventral posterior thalamus. J Neurol Neurosurg Psychiatry. 2012; 83(8): 776–784. [PubMed: 22696587]

Krubitzer L, Clarey J, Tweedale R, Elston G, Calford M. A redefinition of somatosensory areas in the lateral sulcus of macaque monkeys. J Neurosci. 1995; 15:3821–3839. [PubMed: 7751949]

Kupers RC, Svensson P, Jensen TS. Central representation of muscle pain and mechanical hyperesthesia in the orofacial region: a positron emission tomography study. Pain. 2004; 108(3): 284–293. [PubMed: 15030948]

Kurth F, Eickhoff SB, Schleicher A, Hoemke L, Zilles K, Amunts K. Cytoarchitecture and probabilistic maps of the human posterior insular cortex. Cereb Cortex. 2010; 20(6):1448–1461. [PubMed: 19822572]

Kuru, M. The Sensory Paths in the Spinal Cord and Brain Stem of Man. Tokyo: Sogensya; 1949. p. 675

Lenz FA, Seike M, Richardson RT, Lin YC, Baker FH, Khoja I, Jaeger CJ, Gracely RH. Thermal and pain sensations evoked by microstimulation in the area of human ventrocaudal nucleus. J Neurophysiol. 1993; 70:200–212. [PubMed: 8360716]

Lenz FA, Seike M, Lin YC, Baker FH, Rowland LH, Gracely RH, Richardson RT. Neurons in the area of human thalamic nucleus ventralis caudalis respond to painful heat stimuli. Brain Res. 1993; 623:235–240. [PubMed: 8221105]

Lenz, FA.; Dougherty, PM. Pain processing in the human thalamus. In: Steriade, M.; Jones, EG.; McCormick, DA., editors. Thalamus, vol II, Experimental and clinical aspects. Amsterdam: Elsevier; 1997. p. 617-652.

Maihofner C, Kaltenhauser M, Neundorfer B, Lang E. Temporo-spatial analysis of cortical activation by phasic innocuous and noxious cold stimuli - a magnetoencephalographic study. Pain. 2002; 100(3):281–290. [PubMed: 12467999]

Mantyh PW. The spinothalamic tract in the primate: a re-examination using wheatgerm agglutinin conjugated to horseradish peroxidase. Neuroscience. 1983; 9(4):847–862. [PubMed: 6688662]

Mazzola L, Isnard J, Peyron R, Guenot M, Mauguiere F. Somatotopic organization of pain responses to direct electrical stimulation of the human insular cortex. Pain. 146; (1–2):99–104.

Mazzola L, Isnard J, Peyron R, Mauguiere F. Stimulation of the human cortex and the experience of pain: Wilder Penfield's observations revisited. Brain. 2012; 135(Pt 2):631–640. [PubMed: 22036962]

Mesulam MM. Tracing neural connections of human brain with selective silver impregnation. Observations on geniculocalcarine, spinothalamic, and entorhinal pathways. Arch Neurol. 1979; 36(13):814–818. [PubMed: 92302]

Mesulam MM, Mufson EJ. Insula of the old world monkey. I. Architectonics in the insulo-orbito-temporal component of the paralimbic brain. J Comp Neurol. 1982; 212:1–22. [PubMed: 7174905]

Montes C, Magnin M, Maarrawi J, Frot M, Convers P, Mauguière F, Garcia-Larrea L. Thalamic thermo-algesic transmission: ventral posterior (VP) complex versus VMpo in the light of a thalamic infarct with central pain. Pain. 2005; 113(1–2):223–232. [PubMed: 15621383]

Olausson H, Ha B, Duncan GH, Morin C, Ptito A, Ptito M, Marchand S, Bushnell C. Cortical activation by tactile and painful stimuli in hemispherectomized patients. Brain. 2001; 124(5): 916–927. [PubMed: 11335694]

Olausson H, Lamarre Y, Backlund H, Morin C, Wallin BG, Starck G, Ekholm S, Strigo I, Worsley K, Vallbo AB, Bushnell MC. Unmyelinated tactile afferents signal touch and project to insular cortex. Nat Neurosci. 2002; 5(9):900–904. [PubMed: 12145636]

Paulus MP, Simmons AN, Fitzpatrick SN, Potterat EG, Van Orden KF, Bauman J, Swain JL. Differential brain activation to angry faces by elite warfighters: neural processing evidence for enhanced threat detection. PLoS One. 2010; 5(4):e10096. [PubMed: 20418943]

Paulus MP, Flagan T, Simmons AN, Gillis K, Kotturi S, Thom N, Johnson DC, Van Orden KF, Davenport PW, Swain JL. Subjecting elite athletes to inspiratory breathing load reveals behavioral and neural signatures of optimal performers in extreme environments. PLoS One. 2012; 7(1):e29394. [PubMed: 22276111]

Perl ER, Whitlock DG. Somatic stimuli exciting spinothalamic projections to thalamic neurons in cat and monkey. Exp Neurol. 1961; 3:256–296. [PubMed: 13734415]

Perl, ER. Pain and nociception. In: Darian-Smith, I., editor. Handbook of Physiology, Section 1, The Nervous System, Volume III, Sensory Processes. Bethesda: American Physiological Society; 1984. p. 915-975.

Peyron R, Frot M, Schneider F, Garcia-Larrea L, Mertens P, Barral FG, Sindou M, Laurent B, Mauguiere F. Role of operculoinsular cortices in human pain processing: converging evidence from PET, fMRI, dipole modeling, and intracerebral recordings of evoked potentials. Neuroimage. 2002; 17(3):1336–1346. [PubMed: 12414273]

Ploner M, Freund HJ, Schnitzler A. Pain affect without pain sensation in a patient with a postcentral lesion. Pain. 1999; 81:211–214. [PubMed: 10353510]

Poggio GF, Mountcastle VB. A study of the functional contributions of the lemniscal and spinothalamic systems to somatic sensibility. Bulletin of the Johns Hopkins Hospital. 1960; 106:266–316. [PubMed: 14433641]

Pritchard TC, Hamilton RB, Morse JR, Norgren R. Projections of thalamic gustatory and lingual areas in the monkey, Macaca fascicularis. J Comp Neurol. 1986; 244:213–228. [PubMed: 3950095]

Pritchard TC, Hamilton RB, Norgren R. Projections of the parabrachial nucleus in the old world monkey. Exp Neurol. 2000; 165:101–117. [PubMed: 10964489]

Qi HX, Lyon DC, Kaas JH. Cortical and thalamic connections of the parietal ventral somatosensory area in marmoset monkeys (Callithrix jacchus). J Comp Neurol. 2002; 443(2):168–182. [PubMed: 11793354]

Ralston HJ III, Ralston DD. The primate dorsal spinothalamic tract: Evidence for a specific termination in the posterior nuclei (Po/SG) of the thalamus. Pain. 1992; 48:107–118. [PubMed: 1738568]

Ralston HJ III. Pain, the brain, and the (calbindin) stain. J Comp Neurol. 2003; 459(4):329–333. [PubMed: 12687702]

Roberts TS, Akert K. Insular and opercular cortex and its thalamic projection in Macaca mulatta. Schweiz Arch Neurol Neurochir Psychiatr. 1963; 92:1–43. [PubMed: 13974330]

Robinson CJ, Burton H. Somatic submodality distribution within the second somatosensory (SII), 7b, retroinsular, postauditory, and granular insular cortical areas of M. fascicularis. J Comp Neurol. 1980; 192:93–108. [PubMed: 7410615]

Rockel AJ, Heath CJ, Jones EG. Afferent connections to the diecephalon in the marsupial phalanges and the question of sensory convergence in the "posterior group" of the thalamus. J Comp Neurol. 1972; 145:105–130. [PubMed: 5036665]

Rose JE, Mountcastle VB. The thalamic tactile region in rabbit and cat. J Comp Neurol. 1952; 97:441–489. [PubMed: 13034930]

Rosenkranz MA, Busse WW, Johnstone T, Swenson CA, Crisafi GM, Jackson MM, Bosch JA, Sheridan JF, Davidson RJ. Neural circuitry underlying the interaction between emotion and asthma symptom exacerbation. Proc Natl Acad Sci U S A. 2005; 102(37):13319–13324. [PubMed: 16141324]

Saper CB. The central autonomic nervous system: Conscious visceral perception and autonomic pattern generation. Annu Rev Neurosci. 2002; 25:433–469. [PubMed: 12052916]

Schlereth T, Magerl W, Treede R. Spatial discrimination thresholds for pain and touch in human hairy skin. Pain. 2001; 92(1–2):187–194. [PubMed: 11323139]

Schmahmann JD, Leifer D. Parietal pseudothalamic pain syndrome: Clinical features and anatomic correlates. Arch Neurol. 1992; 49:1032–1037. [PubMed: 1417510]

Schmued L, Kyriakidis K, Heimer L. In vivo anterograde and retrograde axonal transport of the fluorescent rhodamine-dextran-amine, Fluoro-Ruby, within the CNS. Brain Res. 1990; 526:127–134. [PubMed: 1706635]

Seth AK, Suzuki K, Critchley HD. An interoceptive predictive coding model of conscious presence. Front Psychol. 2011; 2:395. Epub;%2012 Jan 10.:395. [PubMed: 22291673]

Small DM. Taste representation in the human insula. Brain Struct Funct. 2010; 214(5–6):551–561. [PubMed: 20512366]

Sprenger T, Seifert CL, Valet M, Andreou AP, Foerschler A, Zimmer C, Collins DL, Goadsby PJ, Tolle TR, Chakravarty MM. Assessing the risk of central post-stroke pain of thalamic origin by lesion mapping. Brain. 2012; 135(Pt 8):2536–2545. [PubMed: 22719000]

Stancak A, Mlynar J, Polacek H, Vrana J. Source imaging of the cortical 10 Hz oscillations during cooling and warming in humans. Neuroimage. 2006; 33(2):660–671. [PubMed: 16952469]

Starr CJ, Sawaki L, Wittenberg GF, Burdette JH, Oshiro Y, Quevedo AS, Coghill RC. Roles of the insular cortex in the modulation of pain: insights from brain lesions. J Neurosci. 2009; 29(9): 2684–2694. [PubMed: 19261863]

Stepniewska I, Sakai ST, Qi HX, Kaas JH. Somatosensory input to the ventrolateral thalamic region in the macaque monkey: potential substrate for Parkinsonian tremor. J Comp Neurol. 2003; 455:378–395. [PubMed: 12483689]

Strigo IA, Duncan GH, Boivin M, Bushnell MC. Differentiation of visceral and cutaneous pain in the human brain. J Neurophysiol. 2003; 89(6):3294–3303. [PubMed: 12611986]

Szabo J, Cowan WM. A Stereotaxic Atlas of the Brain of the Cynomolgus Monkey (Macaca fascicularis). The Journal of Comparative Neurology. 1984; 222:265–300. [PubMed: 6365984]

Tasker, RR. Stereotaxic surgery. In: Wall, PD.; Melzack, R., editors. Textbook of Pain. Edinburgh: Churchill Livingstone; 1984. p. 639-655.

Veldhuijzen DS, Greenspan JD, Kim JH, Lenz FA. Altered pain and thermal sensation in subjects with isolated parietal and insular cortical lesions. Eur J Pain. 2010; 14(5):535–511. [PubMed: 19939715]

Veldhuizen MG, Bender G, Constable RT, Small DM. Trying to detect taste in a tasteless solution: modulation of early gustatory cortex by attention to taste. Chem Senses. 2007; 32(6):569–581. [PubMed: 17495173]

Veldhuizen MG, Albrecht J, Zelano C, Boesveldt S, Breslin P, Lundstrom JN. Identification of human gustatory cortex by activation likelihood estimation. Hum Brain Mapp. 2011; 32(12):2256–2266. [PubMed: 21305668]

Vierck CJ, Whitsel BL, Favorov OV, Brown AW, Tommerdahl M. Role of primary somatosensory cortex in the coding of pain. Pain. 2013; 154:334–344. [PubMed: 23245864]

Voets NL, Adcock JE, Flitney DE, Behrens TE, Hart Y, Stacey R, Carpenter K, Matthews PM. Distinct right frontal lobe activation in language processing following left hemisphere injury. Brain. 2006; 129(Pt 3):754–766. [PubMed: 16280351]

Vogel H, Port JD, Lenz FA, Solaiyappan M, Krauss G, Treede RD. Dipole source analysis of laser-evoked subdural potentials recorded from parasylvian cortex in humans. J Neurophysiol. 2003; 89(6):3051–3060. [PubMed: 12783950]

Wall PD. Pain in the brain and lower parts of the anatomy. Pain. 1995; 62:389–391. [PubMed: 8657442]

Wang GJ, Tomasi D, Backus W, Wang R, Telang F, Geliebter A, Korner J, Bauman A, Fowler JS, Thanos PK, Volkow ND. Gastric distention activates satiety circuitry in the human brain. Neuroimage. 2008; 39(4):1824–1831. [PubMed: 18155924]

Welker WI, Johnson JI Jr, Pubols BH Jr. Some morphological and physiological characteristics of the somatic sensory system in raccoons. Am Zool. 1964; 4:75–94. [PubMed: 14135028]

Whitsel BL, Favorov OV, Li Y, Quibrera M, Tommerdahl M. Area 3a neuron response to skin nociceptor afferent drive. Cereb Cortex. 2009; 19:349–366. [PubMed: 18534992]

Williamson JW, Nobrega AC, McColl R, Mathews D, Winchester P, Friberg L, Mitchell JH. Activation of the insular cortex during dynamic exercise in humans. J Physiol. 1997; 503(Pt 2): 277–283. [PubMed: 9306272]

Willis WD, Trevino DL, Coulter JD, Maunz RA. Responses of primate spinothalamic tract neurons to natural stimulation of hindlimb. J Neurophysiol. 1974; 37:358–372. [PubMed: 4205568]

Willis WD, Kenshalo DR Jr, Leonard RB. The cells of origin of the primate spinothalamic tract. J Comp Neurol. 1979; 188:543–574. [PubMed: 118192]

Willis WD Jr, Zhang X, Honda CN, Giesler GJ Jr. Projections from the marginal zone and deep dorsal horn to the ventrobasal nuclei of the primate thalamus. Pain. 2001; 92(1–2):267–276. [PubMed: 11323148]

Willis WD Jr, Zhang X, Honda CN, Giesler GJ Jr. A critical review of the role of the proposed VMpo nucleus in pain. J Pain. 2002; 3(2):79–94. [PubMed: 14622792]

Wilson LB, Andrew D, Craig AD. Activation of spinobulbar lamina I neurons by static muscle contraction. J Neurophysiol. 2002; 87(3):1641–1645. [PubMed: 11877534]

Yu XH, Zhang ET, Craig AD, Shigemoto R, Ribeiro-da-Silva A, De Koninck Y. NK-1 receptor immunoreactivity in distinct morphological types of lamina I neurons of the primate spinal cord. J Neurosci. 1999; 19:3545–3555. [PubMed: 10212314]

Zhang X, Davidson S, Giesler GJ Jr. Thermally identified subgroups of marginal zone neurons project to distinct regions of the ventral posterior lateral nucleus in rats. J Neurosci. 2006; 26(19):5215–5223. [PubMed: 16687513]

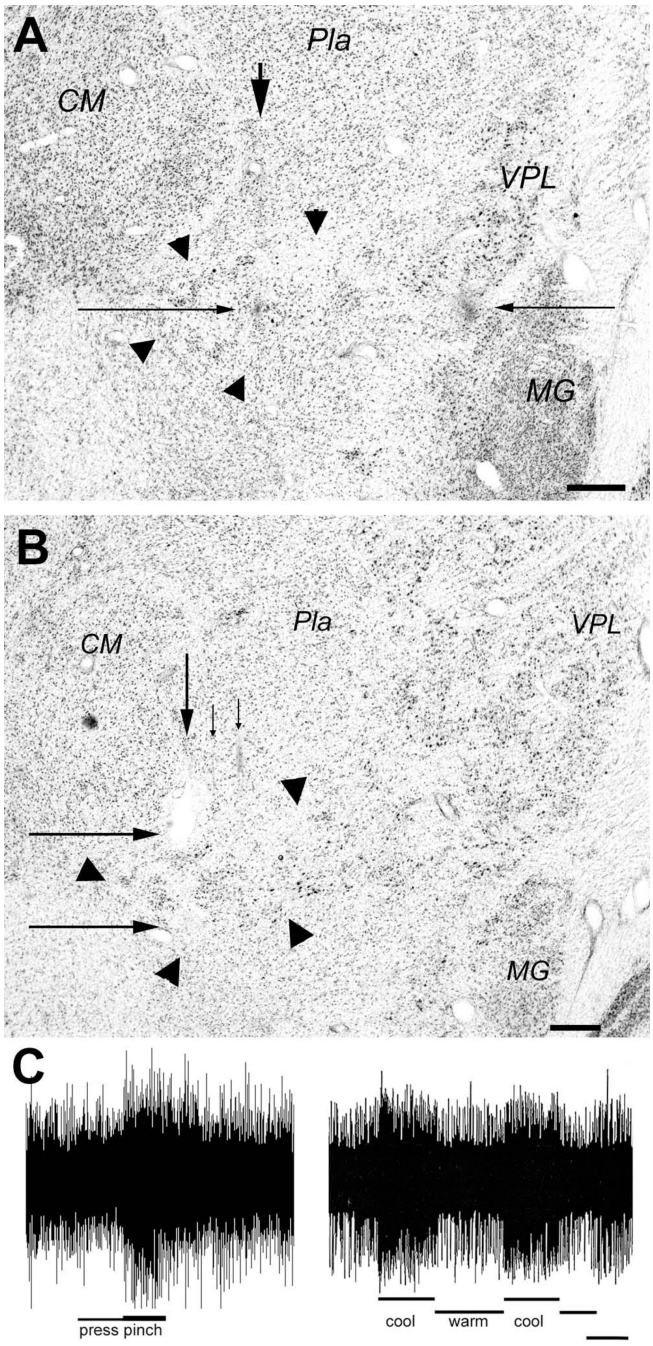

Figure 1.

Evidence verifying the localization of selectively nociceptive or thermoreceptive units and clusters in VMpo. (**A**) shows a photomicrograph of a thionin-stained coronal section from case m30 (on Dec. 17, 1992). The arrow at the top indicates the vertical gliotic trace of the micro-pipette used to make a micro-injection of CTb at the dark spot indicated by the long thin arrow from the left. That spot is at the same depth as the gliotic lesion burned with the microelectrode in a penetration 2 mm further lateral, which is marked by the long thin arrow from the right. That equivalence verifies that the recordings described in the text were made

within the cytoarchitectonic boundaries of VMpo, which are delimited by the large arrowheads. Bar=0.5 mm. (**B**) shows a photomicrograph of a coronal section from case vm1. The arrows at the top that point downwards indicate the histological traces of three microelectrode penetrations in which recordings from selectively nociceptive neurons were obtained. The larger arrow at the top indicates the trace in which two lesions were made, first at the lower border and immediately afterwards a larger one at the upper border of the region in which these recordings were obtained. The long thin arrows from the left indicate the two lesions, which in fact lie at the boundaries of VMpo, as delimited by the large arrowheads. Bar=0.5 mm. (C) shows sample recordings from multi-unit clusters in VMpo responsive selectively to pinch (left, case m30, at the depth of the spot in panel **A**, RF = lateral upper lip, total bar length = 4 sec) or to cool (right, case mop2, RF = medial glabrous hand, bar = 2 sec). Abbreviations: CM, centre median; MG, medial geniculate; Pla, anterior pulvinar; VPL, ventral posterior lateral nucleus.

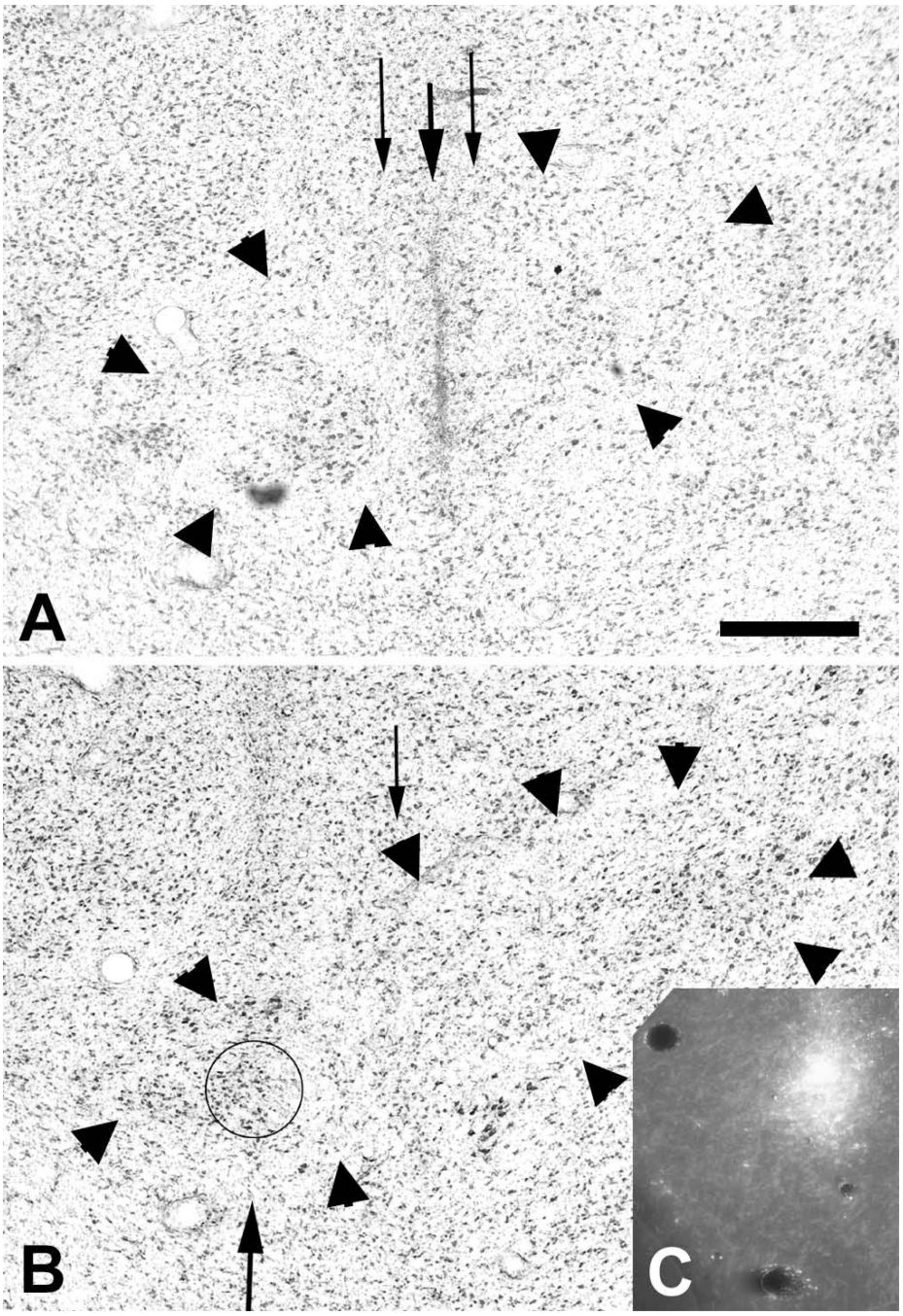

Figure 2.

Evidence of barriers to the precise placement of tracer micro-injections in VMpo. The photomicrographs show the histological traces of microelectrode penetrations #7 and #8 (**A**) and #9 (**B)** in case m36, where the recordings described in the text were obtained. The histological trace of the micro-pipette used to make an iontophoretic micro-injection of Gdx is visible in (**A**), and the trace of the Rdx micro-pipette is visible in (**B**), while (**C**) shows the Rdx micro-injection and a faint histological trace of microelectrode penetration #9. The Gdx injection site was barely 200 μm medial to the intended target, but almost no tracer was

deposited. The Rdx micro-injection is visible and produced good cortical labeling, but it was placed 500 μm medial to the intended target; nevertheless, it was still within the confines of VMpo (delimited by the large arrowheads). Bar=0.5 mm.

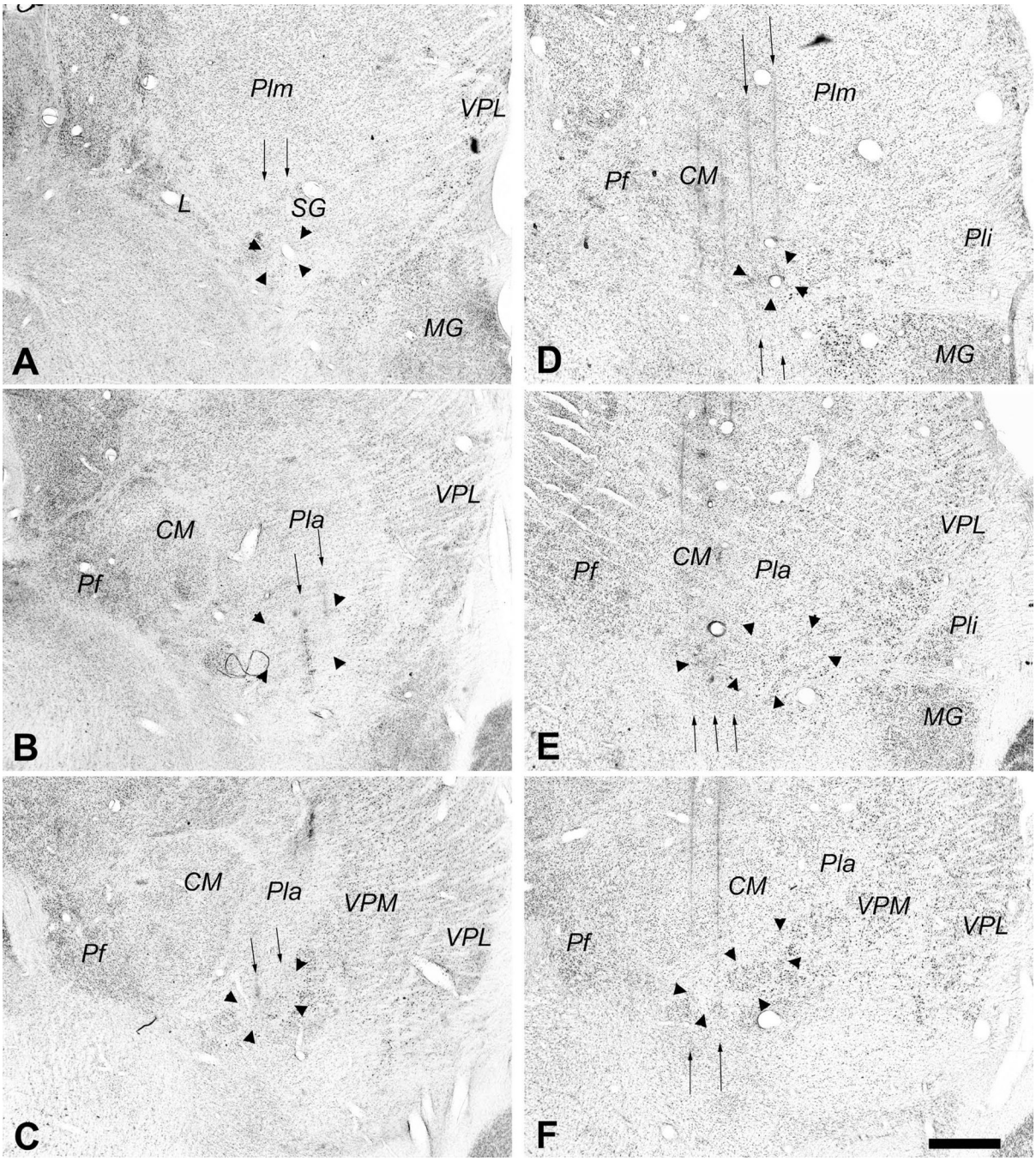

Figure 3.

Photomicrographs of coronal sections showing the histological traces of the microelectrode penetrations made in case m154 (left, panels **A, B, C**) and in case m57 (right, panels **D, E, F**). The borders of VMpo are indicated by large arrowheads. In each case, these photomicrographs show that penetrations were made through a very posterior level of VMpo (top panels, **A, D**), the middle of VMpo (middle panels, **B, E**), and a very anterior level of VMpo (bottom panels, **C, F**). The penetrations in which recordings were obtained from selectively nociceptive or thermoreceptive units and clusters are indicated by the thin

vertical arrows, and the histology shows that these penetrations passed through VMpo. Bar = 0.5 mm. Abbreviations: CM, centre median; L, nucleus limitans; MG, medial geniculate; Pf, parafascicular nucleus; Pla, anterior pulvinar; Pli, inferior pulvinar; Plm, medial pulvinar; SG, supragenicular nucleus; VPL, ventral posterior lateral nucleus; VPM, ventral posterior medial nucleus.

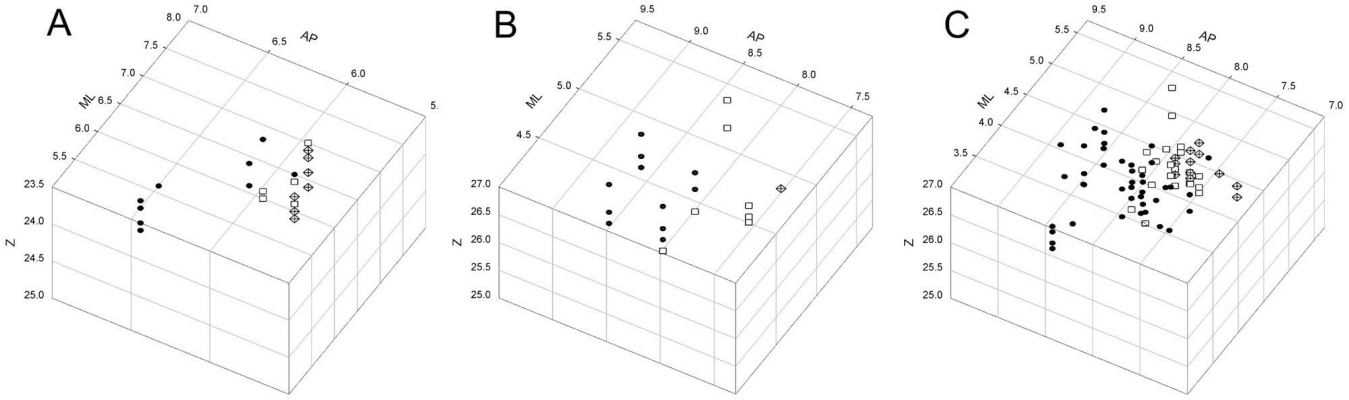

Figure 4.

Three-dimensional graphs showing the topographic stereotaxic distribution of selectively nociceptive units and clusters recorded in VMpo . (**A**) shows case m154 and (**B**) shows case m57, the two cases for which histological evidence is shown in Figure 3 (**C**) shows a collation of five cases (m57, m65, m86, m154, and m177), in which the geometric means were aligned for the recordings with RFs on the hand in each case. Units and clusters with RFs in region 1 (face, head, ear and neck) are indicated by filled circles, in region 2 (hand, arm, shoulder, and chest) by open squares, and in region 3 (foot, leg, abdomen, rump, and tail) by crossed diamonds. The vertical dimension indicates recording depth, the left top angled dimension the Medio-Lateral stereotaxic coordinate, and the right top angled dimension the Antero-Posterior coordinate, all in units of millimeters.

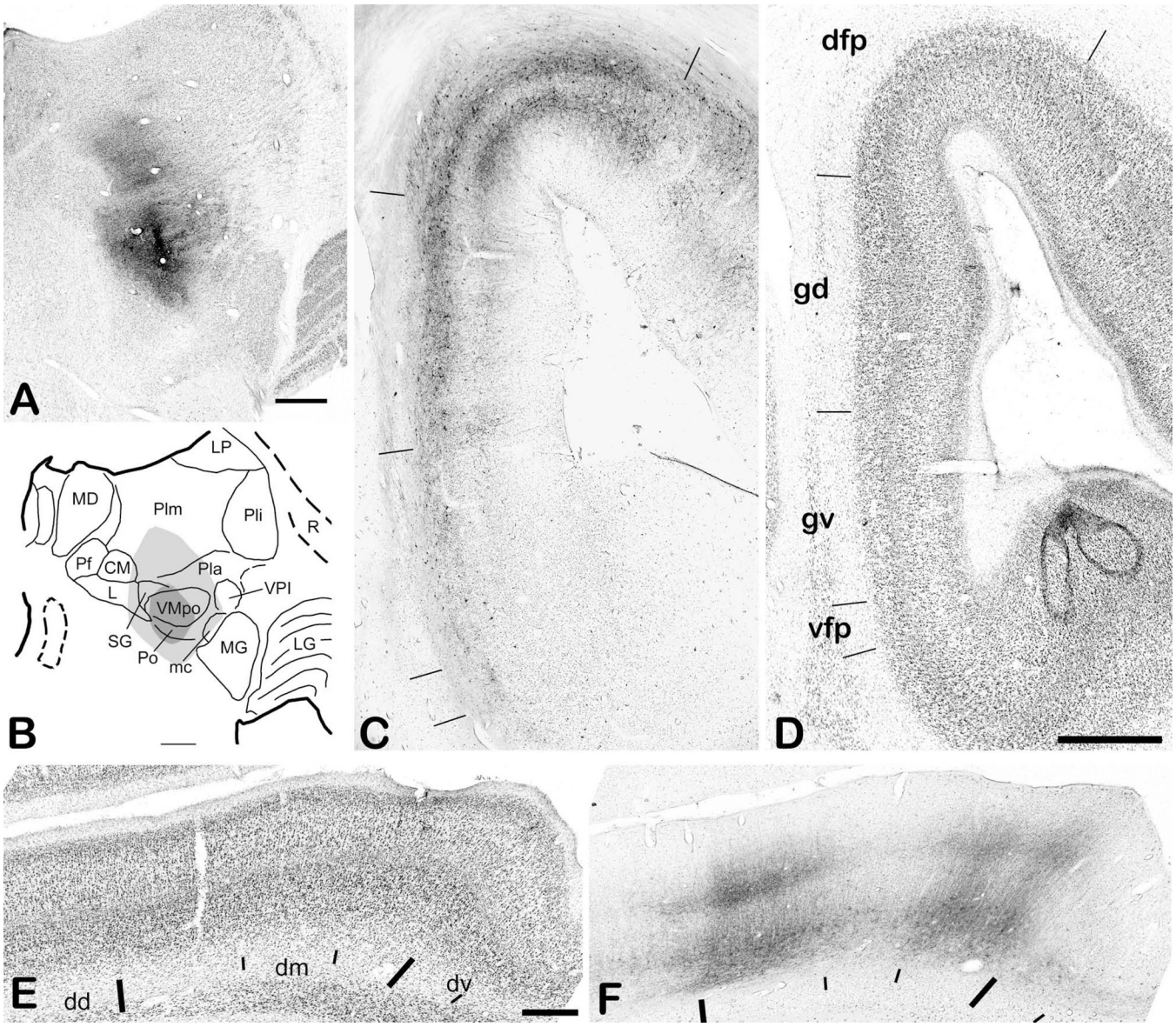

Figure 5.

Representative insular cortical labeling following a large CTb injection centered in VMpo. (**A**) shows a photomicrograph of the injection site. (**B**) shows a drawing of its location in thalamus. (**C**) shows a photomicrograph of the anterograde and retrograde labeling in insular cortex in section 19b, for which a drawing is shown in the top panel of Figure 6, and (**D**) shows the adjacent thionin-stained section. The tick marks in (**C**) mark sharp changes in the pattern and density of the labeling in the middle layers, and they correspond well with the locations of the tick marks in (**D**), which delimit cytoarchitectonically distinct insular cortical areas as identified in the companion article (Evrard et al., xxxx; the initial capital I is suppressed). Panels (**E**) and (**F**) show another pair of adjacent CTb-labeled (#15a) and thionin-stained sections from a more anterior level, between sections 14c and 15b in the top panel of Figure 6 and equivalent to A15.5 in the bottom panel of Figure 6. Bar=1 mm (**C, D**), 0.5 mm (**E, F**). Abbreviations: CM, centre median; dd, dorsal dysgranular area of insula;

dm, mound dysgranular area of insula; dv, ventral dysgranular area of insula; gd, dorsal granular area of insula; gv, ventral granular area of insula; L, nucleus limitans; LG, lateral geniculate; LP, lateral posterior nucleus; mc, magnocellular part of the medial geniculate; MD, medial dorsal nucleus; MG, medial geniculate; Pf, parafascicular nucleus; Pla, anterior pulvinar; Pli, inferior pulvinar; Plm, medial pulvinar; R, reticular nucleus; SG, supragenicular nucleus; vfp, posterior ventral fundus of insula; VMpo, posterior part of the ventral medial nucleus; VPI, ventral posterior inferior nucleus.

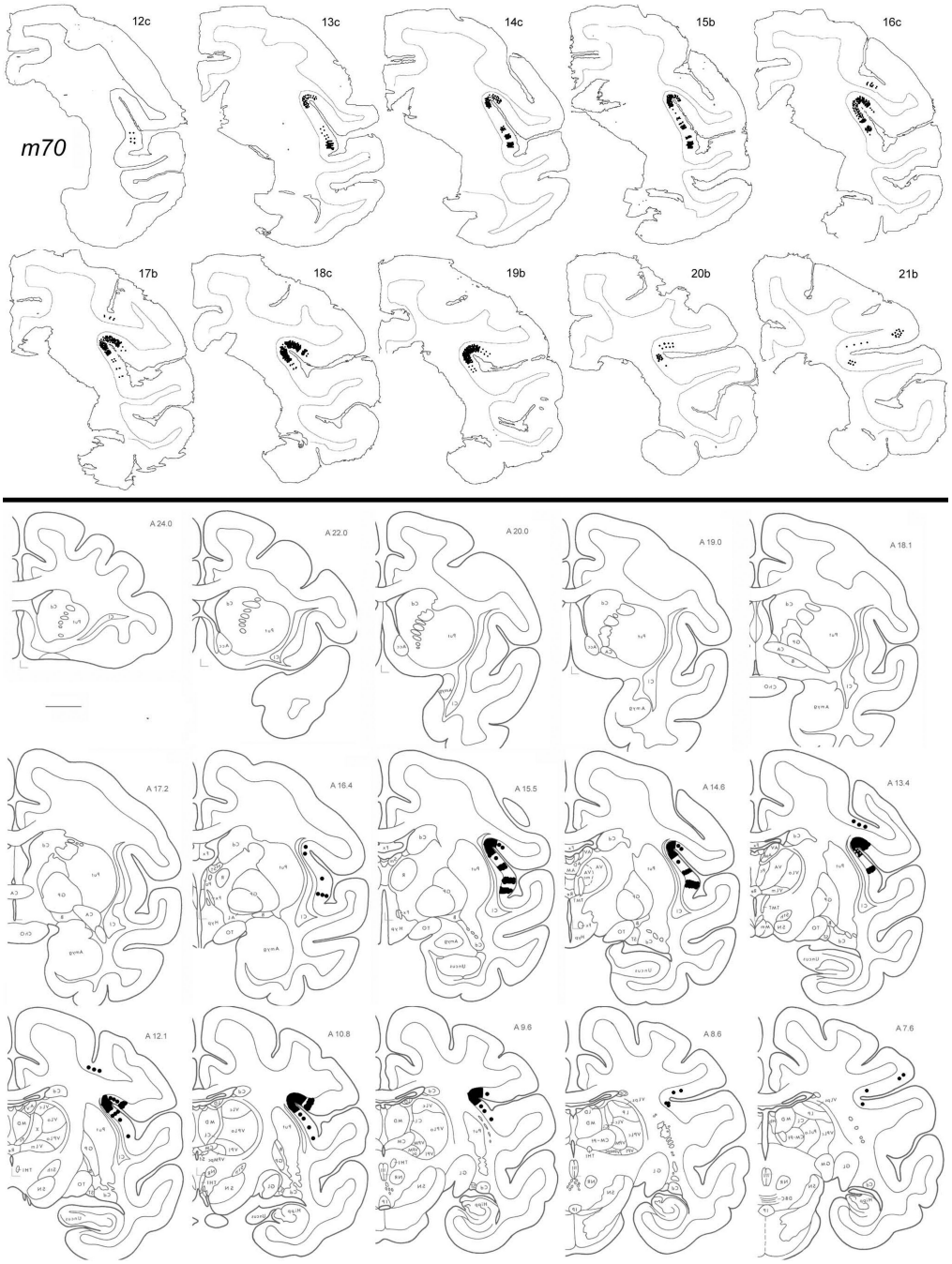

Figure 6.

The anterograde middle-layer terminal labeling in the cortex of case m70, shown on the original plotted sections in a coronal series from anterior (top row, left) to posterior (second row, right) sections (top) and also transposed onto the standardized series that was used to collate all cases with anterograde labeling over the entire antero-posterior extent of insular cortex (taken with permission from the atlas of the macaque monkey brain by Szabo and Cowan, 1984). Bar = 5 mm.

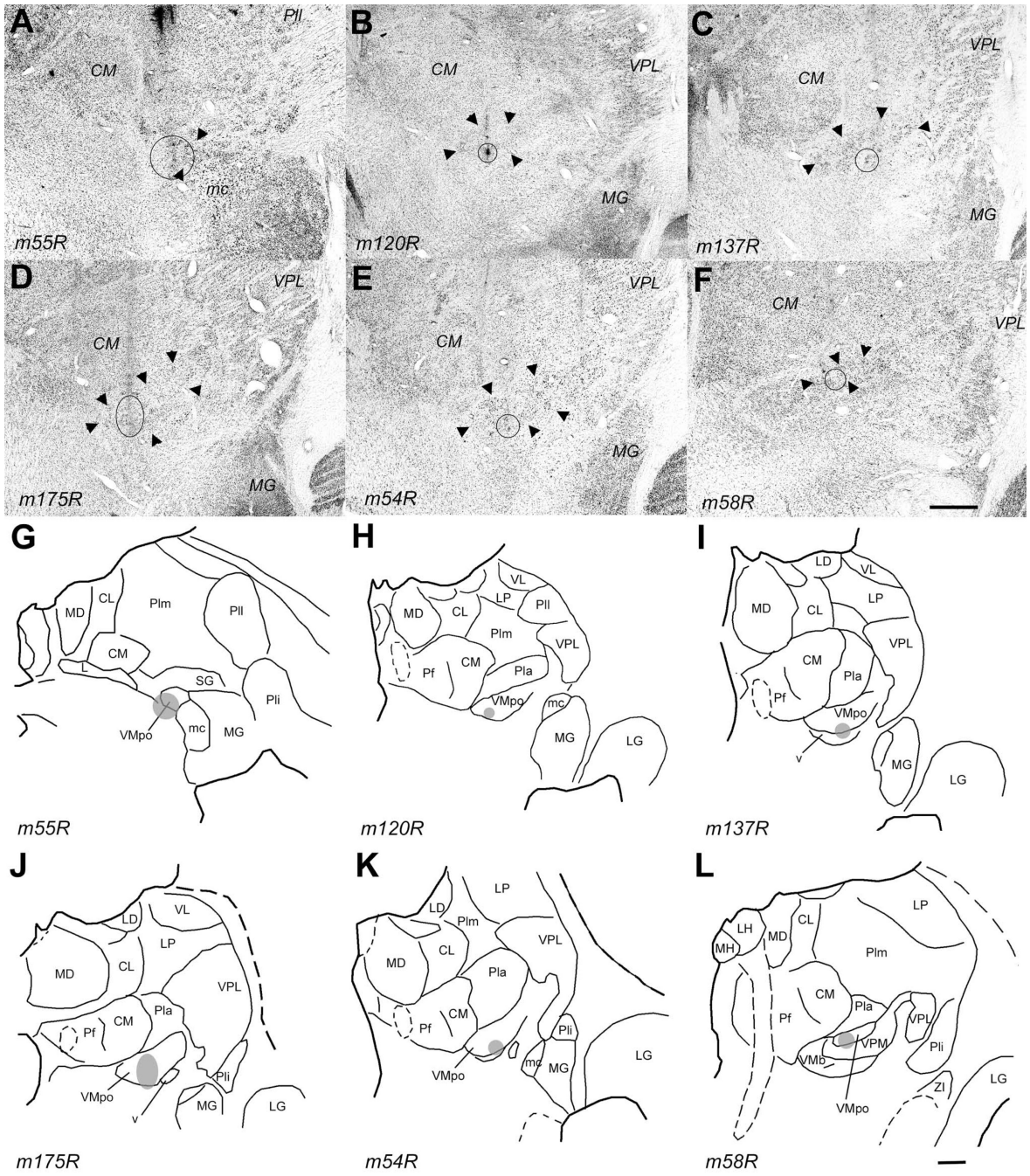

Figure 7.

The injection sites in the six cases that demonstrate the topographic organization of the VMpo projection to dorsal posterior insular cortex. The top panel (**A – F**) shows for each case a photomicrograph of the coronal thionin-stained section in which the histological trace of the micro-pipette and the micro-injection placement are best seen. A solid circle or oval indicates the outline of the micro-injection , as seen in that or an adjacent (fluorescent) section; the large arrowheads indicate the cytoarchitectonic boundaries of VMpo. The lower panel (**G – L**) shows for each case a line drawing of the section shown above; together,

these demonstrate the placement of each micro-injection at a different antero-posterior level of VMpo, progressing from a very posterior level (upper left, **A** and **G**, case m55R) to a very anterior level (lower right, **F** and **L**, case m58R). Bar = 1 mm for both. Abbreviations: CL, central lateral nucleus; CM, centre median; L, nucleus limitans; LD, lateral dorsal nucleus; LG, lateral geniculate; LH, lateral habenula; LP, lateral posterior nucleus; mc, magnocellular part of the medial geniculate; MD, medial dorsal nucleus; MG, medial geniculate; MH, medial habenula; Pf, parafascicular nucleus; Pla, anterior pulvinar; Pli, inferior pulvinar; Plm, medial pulvinar; R, reticular nucleus; SG, supragenicular nucleus; VL, ventral lateral nucleus; VMpo, posterior part of the ventral medial nucleus; VPL, ventral posterior lateral nucleus; VPM, ventral posterior medial nucleus.

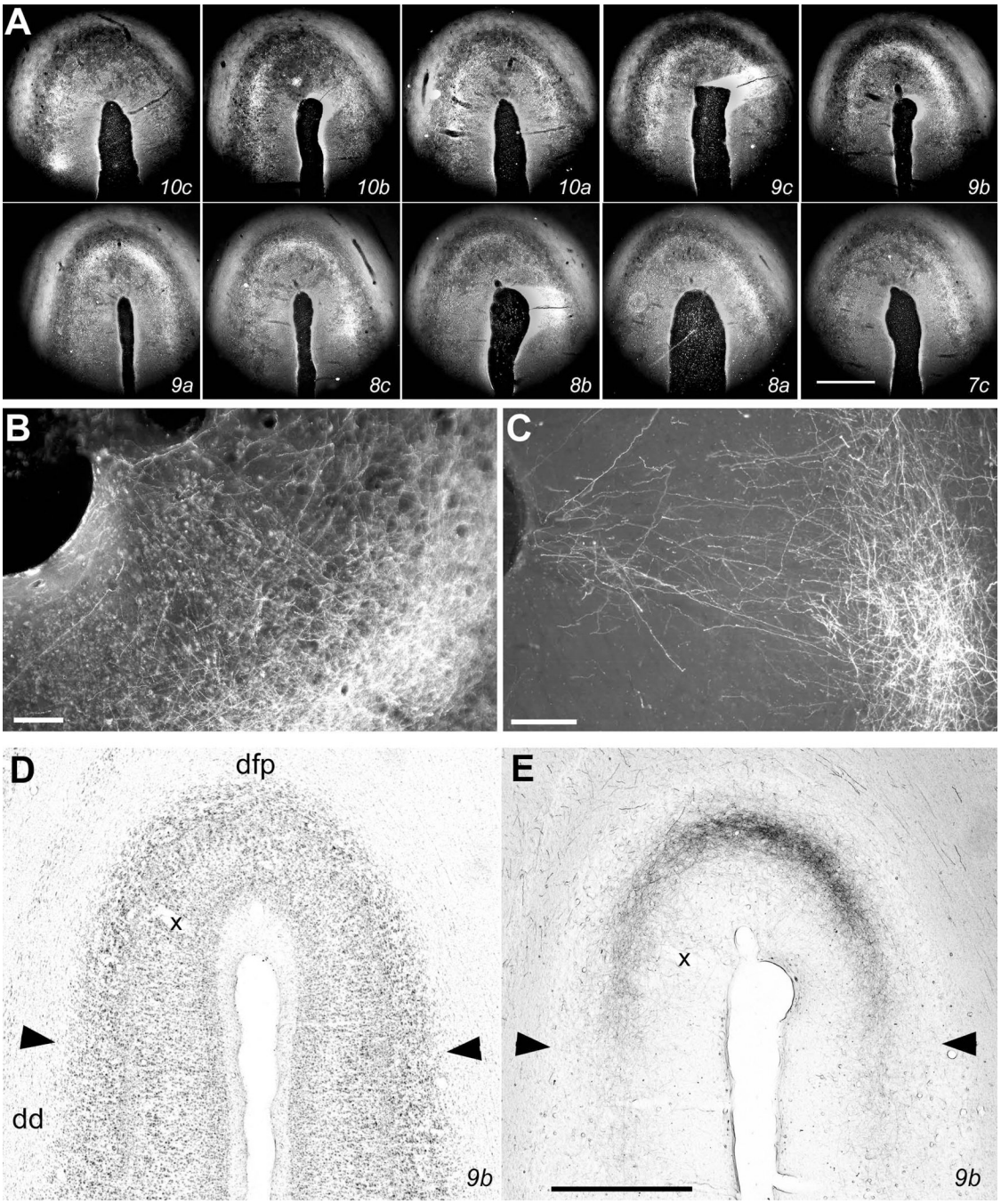

Figure 8.

Photomicrographs of labeling in Idfp. (**A**) shows darkfield photomicrographs of every consecutive 1-in-5 section from case m54R, from posterior (upper left, section *10c*) to anterior (lower right, section *7c*), in order to document the spiral pattern of labeling across the fundus of the SLS. The section numbers correspond with the levels shown in the coronal drawings in Figure 9. The bright middle-layer terminal labeling is most dense in the ventral aspect of the medial wall in *10c* and at a more dorsal location in *10b*; it extends across the fundus in sections *9c–a*, is dense in the lateral wall in sections *8c–a*, and wanes in the lateral

wall with almost no labeling remaining in the medial wall and fundus in *7c*. (**B**) shows at higher magnification the labeling in the lateral portion of the fundus in section *9b*. The labeling is dense in layers 3b-4, and axons with boutons can be seen in the supragranular layers, including layer 1. (The vessel entering at approximately the center of the fundus can be seen both in (A) and at the upper left in (**B**).) (**C**) shows the supragranular labeling more clearly from a triple-labeling case (m178, 10K dextran coupled to Alexa 546) that will be described in detail in a subsequent report. (**D, E**) show bright-field photomicrographs of the adjacent thionin and the CTb-labeled sections numbered #9b. The labeling extends continuously across the fundus between the medial and lateral borders of Idfp, which are indicated by the arrowheads. (The borders are clearly visible, in spite of the ice artifact that mars this thionin section. The potential sub-partition at the center of the fundus that is described in the companion article is also obvious.) Bar = 1 mm (**A, D, E**), 0.1 mm (**B, C**).

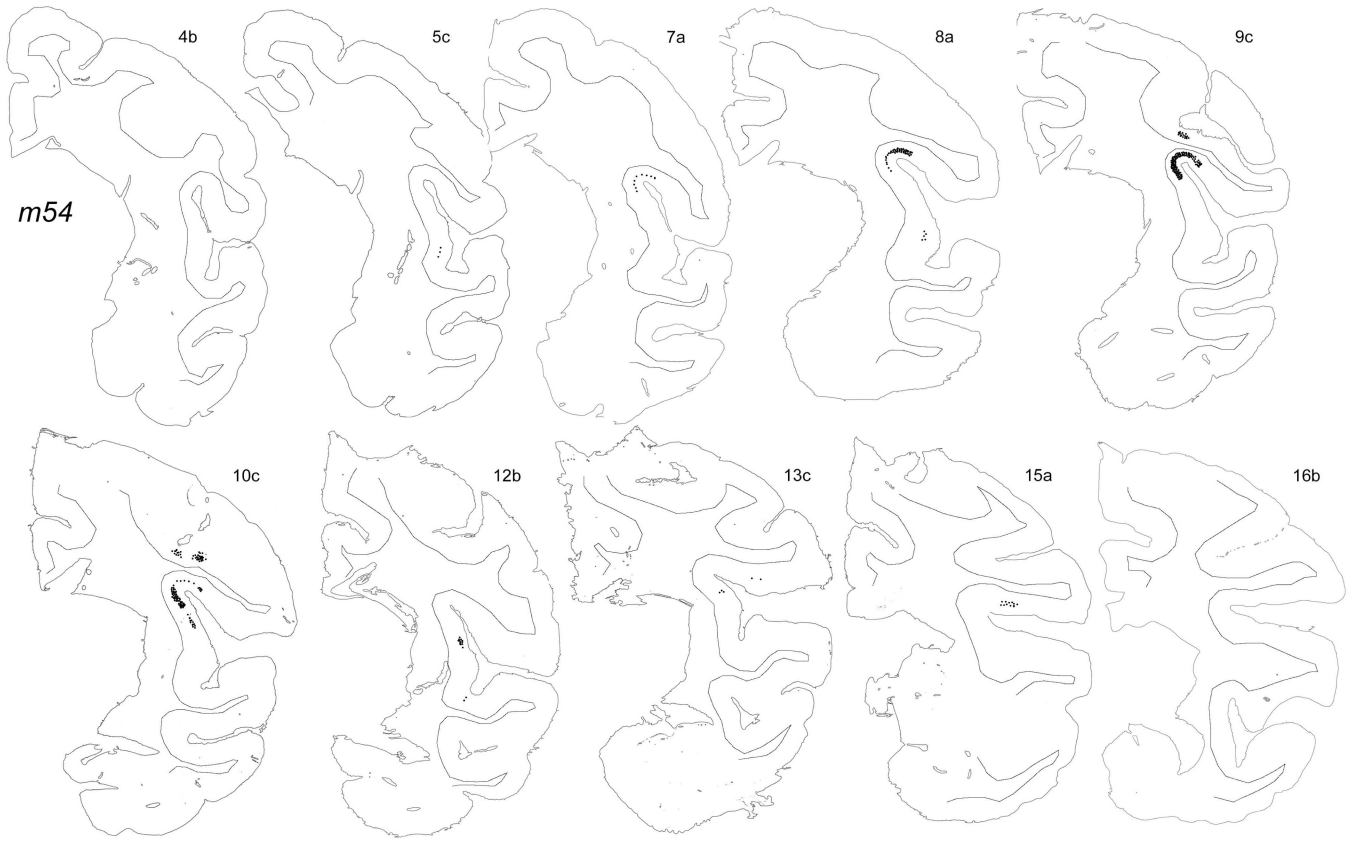

Figure 9.

Original plots showing the distribution of labeling in case m54R on the outlines of the individual named sections. The labeling in the dorsal bank of the LS shown in section 15a does not originate from VMpo. Top left most anterior, bottom right most posterior. Bar = 5 mm.

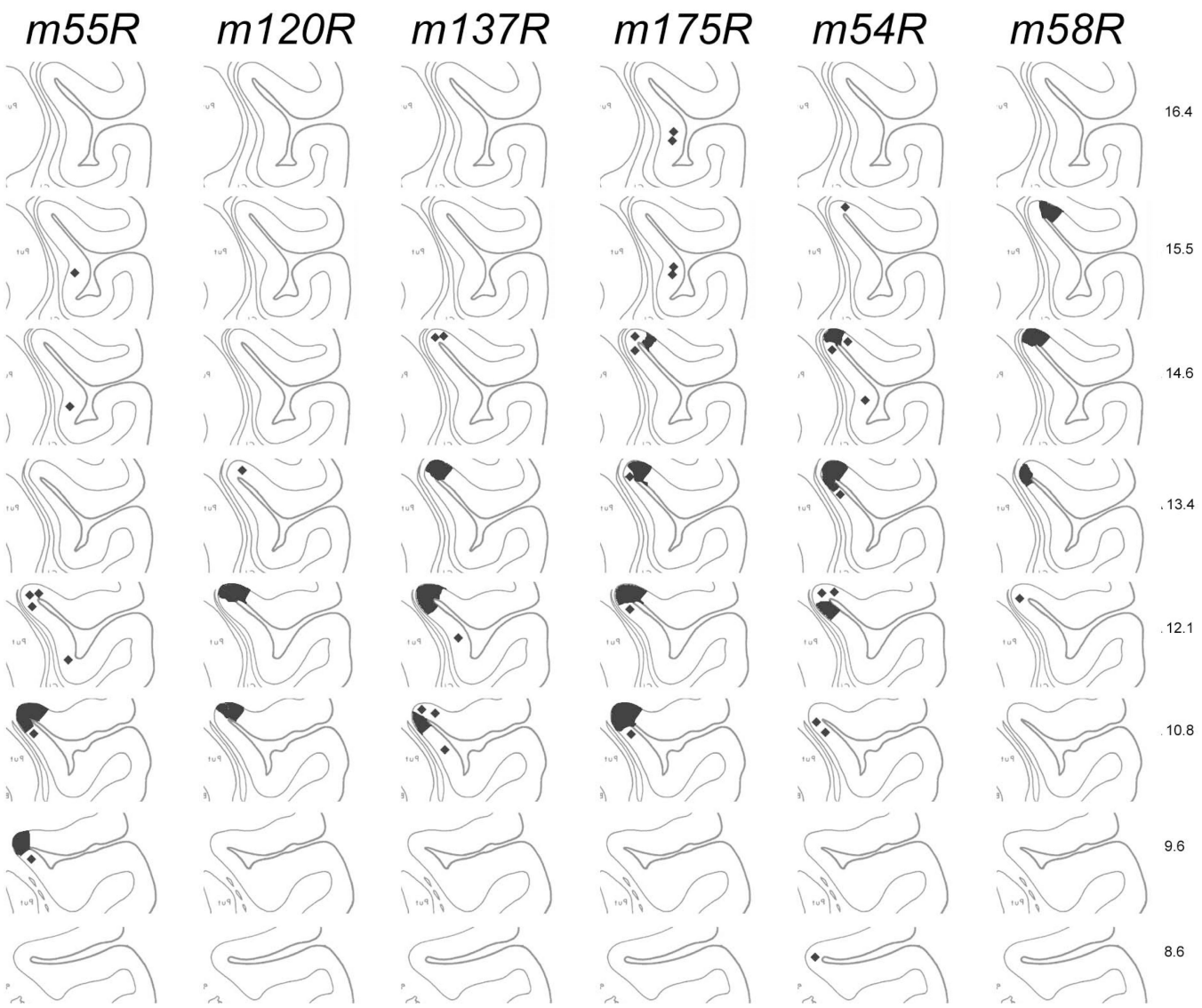

Figure 10.

The topographic distribution of VMpo projections to Idfp is shown by representations of the labeling observed in six cases on a standard composite of line drawings, extracted from the drawings of Szabo and Cowan (1984) at the indicated levels. Only the posterior half of insular cortex is shown.

Table 1

Details for Six Cases Showing Topography of VMpo Projection to Idfp

Case	Tracer	Survival	Inj location	Term location	Term range
m55R	BDA	19d	3/16 = 19%	5/45=11%	3–7 = 7–16%
m120R	Gdx	29	4/16 = 25%	10/52 = 19%	7–13 = 14–25%
m137R	Rdx	28	6/13 = 46%	13/49 = 27%	9–17 = 18–35%
m175R	LYdx (40nL)	22	9/12 = 75%	27/80 = 34%	16–38 = 20–48%
m54R	BDA	21	9/11 = 82%	20/43 = 46%	13–27 = 30–63%
m58R	Rdx	22	11/12 = 92%	16/30 = 53%	12–20 = 40–67%